ORGANIC AND ELEMENTAL CARBON SIZE DISTRIBUTIONS OF LOS ANGELES AEROSOLS MEASURED DURING SCAQS

Final Report to

The Coordinating Research Council
219 Perimeter Center Parkway
Atlanta, GA 30346

CRC Project No. SCAQS–6–1

and

The California Air Resources Board
1102 Q Street
P.O. Box 2815
Sacramento, CA 95812

CARB Contract No. A732–075

Submitted by

Peter H. McMurry
Department of Mechanical Engineering
University of Minnesota
111 Church St. SE
Minneapolis, MN 55455

August, 1989

Revised December, 1989

Particle Technology Laboratory No. 713

TABLE OF CONTENTS

ABSTRACT 2

INTRODUCTION 3

EXPERIMENTAL

SAMPLE HANDLING AND ANALYSIS PROCEDURES 3

Substrates and Substrate Preparation 3
Sample Storage 3
Sample Analysis 4

DATA REDUCTION 4

Blank Correction and Uncertainty Estimates 4
Tabulated Data 5
MOUDI Size–Dependent Efficiencies and Data Inversion 5

RESULTS AND DISCUSSION 6

Uninverted Data 6
Inverted Data 13
Comparisons with Other Samplers 31

ACKNOWLEDGMENTS 36

REFERENCES 36

APPENDICES

I. Summary of MOUDI Samples Acquired During SCAQS 37
II. Size–dependent Collection Efficiencies 42
III. Loadings on MOUDI Stages for SCAQS Measurements 47
IV. Lognormal Fits to SCAQS Data 65

ABSTRACT

This report summarizes measurements of size–resolved residual organic carbon (ROC) and elemental carbon (EC) made by researchers from the University of Minnesota during the Southern California Air Quality Study (SCAQS). Measurements were made with MOUDI impactors. Impactors were located at Claremont and Rubidoux during summer SCAQS sampling, and at Long Beach and Los Angeles during the fall.

It was found that the average mass mean diameter of ROC ranged from 0.43 μm at Los Angeles to 0.62 μm at Rubidoux. Mass mean diameters of EC were systematically smaller than for ROC, ranging from 0.39 μm at Los Angeles to 0.45 μm at Rubidoux. The Rubidoux ROC mean sizes were systematically and substantially larger than sizes at the other three sites.

The ROC/EC ratio varied with site, season, and particle size. Average ROC/EC ratios were 2.66 (Claremont), 2.12 (Rubidoux), 1.51 (Long Beach) and 1.26 (Los Angeles). Although there was no systematic dependence of ROC/EC ratios with particle size, there was a tendency for values to be higher for particles at the large ($\simeq$ 1 μm) and small ($\simeq$0.05–0.1 μm) extremes of the measured size spectrum.

The data were 'inverted' to account for the effect of size–dependent collection efficiencies on measured size distributions. All data were inverted with two inversion schemes: the modified Twomey routine developed by Walter John and coworkers at the Air and Industrial Hygiene Laboratory (Berkeley, CA), and the MICRON code developed by Wolfenbarger and Seinfeld (Caltech). Integral moments of inverted size distributions obtained with these two inversion schemes were compared. It was found that for the integral moment corresponding to particle mass (the 3rd moment) the two inversion methods were in good agreement. This is not surprising since the techniques are constrained to return the measured mass. However, for smaller or larger moments the integral moments can be up to several orders of magnitude different. Although resolving differences between inversion schemes is beyond the scope of the present research, the discrepancies in integral moments is a serious concern. Because size distributions are usually measured with the objective of calculating some integral moment (light scattering or absorption, dry deposition, lung deposition, etc.), it is essential to have some means of estimating most likely values and uncertainties of such integrals. This result suggests that uncertainties for integrals other than total mass can be large.

A limited number of comparisons between EC concentrations obtained with the MOUDI with other samplers was done for the Claremont site. As with previous studies it is found that correlations are poor, with R^2 values ranging down to 0.35. MOUDI EC data were found to be somewhat better correlated with the Ford Spectrometer (an optical absorption device) data than with data from a quartz filter. A similar result was found during the 1986 Carbonaceous Species Methods Comparison Study where the MOUDI agreed best with the LBL aethalometer, another optical absorption device. McMurry and Zhang (Aerosol Sci. Technol. 10:430–437) discussed discrepancies for carbon measurements among different samplers and conclude that impactors may be superior to filters for sampling carbon–containing particulate matter.

INTRODUCTION

Particle size plays a sensitive role in atmospheric aerosol phenomena including optical extinction, dry deposition, and cloud nucleation. In order to evaluate the contributions of various chemical species to these effects, it is important to have information on size–resolved chemical composition. the measurements of organic and elemental carbon size distributions discussed in this paper were made with the objective of improving our understanding of such phenomena. Measurements were made with two microorif(MOUDIs) (1) during the Southern California Air Quality Study (SCAQS). Samples were analyzed for elemental and organic carbon by Dr. Kochy Fung and coworkers at ERT, Inc (2). Objectives of these measurements are to elucidate the role of organic and elemental carbon in phenomena including dry deposition and optical extinction, and to investigate the evolution of secondary organic aerosols by gas to particle formation in the atmosphere.

The use of MOUDIs to measure organic and elemental carbon size distributions has been discussed previously (3). The interested reader is referred to that previous paper for a more detailed discussion of measurement procedures and sampling artifacts with MOUDI and filter samplers.

EXPERIMENTAL

MOUDIs were located at Claremont and Rubidoux, CA during summer–SCAQS intensive sampling days and at Long Beach and Los Angeles during fall–SCAQS intensive sampling days. The nominal sampling period for daytime measurements was four hours (06:00–10:00, 10:00–14:00, 14:00–18:00), while a twelve hour period was used at night (18:00–6:00) except on the last day of sampling intensives when sampling was stopped at 1:00. Summer samples were collected on a total of eleven days (June 19, 24, 25, July 13, 14, 15, Aug. 27, 28, 29, Sept 2, 3, 1989) and fall samples were collected on a total of six days (Nov 11, 12, 13, Dec. 3, 10, 11). A summary of information on all samples collected with MOUDIs during SCAQS is included in Appendix I.

The MOUDIs were preceded by cyclones (4) to remove particles larger than about 2 μm. A total of eight impaction stages was used with nominal 50% cut points ranging from 0.04 to 3.2 μm. Detailed information on size–dependent collection efficiencies for each stage is given in Appendix II. Particles were collected by inertial impaction on ungreased aluminum foil substrates. The foils were precleaned by baking for 3 hours at 600 °C in air.

SAMPLE HANDLING AND ANALYSIS PROCEDURES

Substrates and Substrate Preparation

Aerosol samples were collected on aluminum foil (impactor stages) or on quartz filters (impactor afterfilter). The aluminum foil was punched from 0.001 inch foil sheets with a 1 7/16 inch punch, and was precleaned by baking for 3 hours at 600 °C in air. The 37 mm Pallflex QAO Quartz afterfilters were precleaned by baking for 2 hours at 700 °C in air.

Sample Storage

After sample collection was completed, samples were transferred to 47 mm petrislides. A stack of 9 petrislides from each MOUDI sample (8 impactor stages and one afterfilter) was wrapped in aluminum foil, enclosed in plastic ziploc bags, and placed in temporary storage in

the freezer in the SCAQS headquarters trailer. The trailers were located at Claremont during the summer intensives and at Long Beach during the Fall. Samples were hand carried on ice to ERT, Inc. twice during the summer and twice during the fall where they were again stored in a freezer until they were analyzed.

Sample Analyses

Samples were analyzed at ERT, Inc. using the technique described by Mueller *et al.* (1982). An aliquot from each sample was loaded into a platinum boat and put into contact with MnO_2 catalyst. The sample was first heated to 525 C in He, and then (with air addition) to 850 C. Carbonaceous material that is released from the sample (mostly as CO_2) is converted to methane and detected with a flame ionization detector. The material that is released at 525 C is defined as residual organic carbon (ROC), while the high temperature carbon is defined as elemental carbon (EC). Only a portion of each substrate was required for analysis, so it was possible to perform replicate analyses on a subset of the samples. Samples were analyzed during the summer and fall of 1988, and results were sent to the University of Minnesota both on floppy disk and in hardcopy form. Our primary contact at ERT was Ms. Amy Taketomo.

DATA REDUCTION

The data from ERT were reduced in our lab by Mr. Mark Anderson, a Carleton College undergraduate. Steps that were involved in data reduction included:

- blank correction
- convert substrate mass loadings to airborne concentrations
- prepare tables of concentration data
- 'invert' MOUDI data to obtain better estimates of true size distributions (two inversion schemes were used for comparison)
- fit inverted size distributions with bimodal lognormal distributions
- prepare tables of inverted size distribution data.

Additional details of this work are provided below.

Blank Correction and Uncertainty Estimates

Blanks were estimated from several different types of information. Field and dynamic blanks were analyzed for EC and ROC loadings. Also, the top impactor stage serves as an excellent dynamic blank. The cyclone located upstream of the MOUDI collects all particles larger than about 2 μm, and the cutpoint of the top impactor stage is 3.2 μm. Therefore, no particles should have been collected on this stage, and visible deposits were not observed. However, this substrate was handled identically to all other substrates, and was exposed to the same gases for the same time period. Therefore the ROC and EC loading on this stage should be representative of blank values for the other stages.

Blank values for ROC and EC during summer and fall SCAQS measurements are summarized in Table I. In estimating blank values for the quartz filters, information from previous field studies with similar filters was used to supplement SCAQS data. The foil blanks are based solely on SCAQS measurements. The blank values in Table I. were subtracted from all loadings reported by ERT, Inc.

Table I. Summary of Blanks (μg/substrate)

	Summer SCAQS	Fall SCAQS
ROC, Aluminum Foil	3.0 ± 3.0	1.5 ± 0.7
ROC, Quartz Afterfilter	7.0 ± 3.0	7.0 ± 3.0
EC, Aluminum Foil	0.0 ± 0.05	0.0 ± 0.1
EC, Quartz Afterfilter	0.1 ± 0.05	0.1 ± 0.05

The variability in the blanks provides a measure of noise in the data. In addition, uncertainties associated with the analytical technique can be determined from replicate analyses of the same substrate. Replicate analyses were performed on 77 foil samples. It was found that variabilities among replicate samples could be approximated by:

$$\text{Replicate Variability for ROC} \approx 0.5 + 0.03*\text{ROC}.$$

$$\text{Replicate Variability for EC} \approx 0.1*\text{EC}.$$

where ROC and EC are the total ROC or EC loadings on the substrates. Based on the variability in the blanks and on variabilities in replicate analyses the following uncertainties for elemental (EC) and organic (ROC) carbon measurements are estimated:

$$\Delta\text{EC } (\mu g/m^3) = (1.0 + 0.05*\text{EC per stage})/V_s$$

$$\Delta\text{ROC } (\mu g/m^3) = (1.0 + 0.05*\text{ROC per stage})/V_s$$

where V_s is the total volume of air sampled. Flow rates (and therefore sample volumes) were accurate to within about 5%.

Tabulated Data

After correcting for blanks, stage loadings were converted to concentrations by dividing by the volume of air sampled. A summary of all data acquired during the study is tabulated in Appendix III. A separate page is included for each intensive sampling day. Data from the upwind sites (Claremont or Long Beach) is shown on the top of the page, and data from the downwind site is shown on the bottom. Two columns are shown for each sample. The first column is for ROC and the second is for EC.

The data in Appendix III were also submitted to the SCAQS data base on floppy disc.

MOUDI Size–Dependent Efficiencies and Data Inversion

For a given input aerosol size distribution, the loading per MOUDI stage depends on the size–dependent collection efficiency for that stage and upstream stages. A zeroth order approximation for determining size distributions from an impactor assumes that all mass collected on a stage is associated with particles having diameters between the 50% cut point (D_{50}) for that stage and the stage immediately upstream. This approach can be used to directly estimate size distributions from the data in Appendix III given the impactor cut points. D_{50}s

for the MOUDIs are included in Appendix II.

A more refined estimate of size distributions measured with impactors can be achieved by taking into account the size–dependent collection efficiencies of each stage. This procedure is commonly referred to as 'data inversion'. Data inversion requires a detailed knowledge of size–dependent collection efficiencies for each stage. The MOUDIs used during SCAQS were calibrated in our laboratory immediately before the program, and a spot check was done between the summer and fall measurements. The MOUDI calibration data that were used to invert the data are summarized in Appendix II.

Several research groups have recently developed schemes for inverting impactor data. We have inverted all of our data using two different inversion schemes: "Twomey" and "MICRON". The Twomey routine was developed Dr. Walter John and coworkers at the Air and Industrial Hygiene Laboratory in Berkeley, CA. The MICRON routine was developed by Mr. Kenneth Wolfenbarger, a Ph.D. candidate working under the supervision of Prof. John Seinfeld at Caltech. These algorithms are mathematically quite different. Our objective in using two schemes was to determine whether the inversion method substantially affects the results.

The Twomey code was used by John and Winklmayr to reduce all of the data for ion size distributions that were collected with the Berner Impactors during SCAQS. Dr. Winklmayr assisted us in adapting their algorithm to the MOUDI impactors. The data inversion program outputs values for the size distribution at 65 particle sizes. These size distributions were fitted with single mode or bimodal lognormal size distributions. Results of these lognormal fits are given in Appendix IV. Again, the lognormal fitting program that was used was developed by Winklmayr in Walter John's group at AIHL, and is the same routine that was used with the ion size–distribution data.

The lognormal results for the Twomey inversions are summarized by site. Two pages are included for each site: one for ROC and one for EC. Again, ASCII files for the data in Appendix IV were submitted to the SCAQS data base. The data in Appendix IV indicate that in some cases the mass in mode 2 is zero. This indicates that a single mode lognormal size was sufficient to account for at least 90% of the mass in the measured distribution.

Mr. Kenneth Wolfenbarger (Caltech) was most helpful in implementing MICRON for inverting our MOUDI data. In the following sections results of the MICRON and Twomey inversions are compared. Tabulated results for the MICRON inversions are not presented.

RESULTS AND DISCUSSION

Uninverted Data

The discussion in this section applies to the 'raw' uninverted data. Size distributions and mean and median sizes are estimated from the impactor d_{50}s.

Average values of EC and ROC mass concentrations are tabulated as a function of time of day in Table II. Note that fall values (Long Beach and Los Angeles) are higher than summer values for this data set.

Mass mean diameters for ROC and EC size distributions are given as a function of time of day in Table III. Note that ROC sizes are systematically greater than EC sizes. Note also that ROC sizes measured at Rubidoux are substantially larger than sizes at other locations.

Table II. Average Mass Concentrations (sum of all stages) Versus Time of Day ($\mu g/m^3$)

Organic Carbon

	6:00–10:00	10:00–14:00	14:00–18:00	18:00–6:00
Summer				
Claremont	7.24±1.25	8.63±3.99	8.33±3.79	4.50±2.21
Rubidoux	5.70±2.24	5.02±3.01	5.08±2.81	3.37±1.25
Fall				
Long Beach	14.62±12.24	7.59±7.44	6.11±5.16	7.29±4.94
Los Angeles	12.32±7.15	7.40±4.61	7.91±4.43	9.53±4.84

Elemental Carbon

	6:00–10:00	10:00–14:00	14:00–18:00	18:00–6:00
Summer				
Claremont	3.44±1.45	3.16±0.95	2.60±0.75	1.61±0.83
Rubidoux	2.93±1.09	2.32±1.80	2.11±2.17	1.71±0.76
Fall				
Long Beach	10.2±6.84	6.11±4.29	4.97±3.44	3.72±1.93
Los Angeles	11.4±6.29	6.12±3.79	5.88±3.36	6.93±3.52

Table III. Average Mass Mean Diameters Versus Time of Day (μm)

Organic Carbon

	6:00–10:00	10:00–14:00	14:00–18:00	18:00–6:00
Summer				
Claremont	0.47±0.09	0.48±0.13	0.46±0.11	0.48±0.12
Rubidoux	0.66±0.21	0.66±0.21	0.59±0.14	0.56±0.15
Fall				
Long Beach	0.49±0.17	0.46±0.13	0.43±0.10	0.46±0.07
Los Angeles	0.36±0.14	0.43±0.16	0.45±0.14	0.47±0.04

Elemental Carbon

Summer				
Claremont	0.36±0.08	0.39±0.09	0.37±0.08	0.38±0.11
Rubidoux	0.44±0.16	0.49±0.19	0.49±0.10	0.38±0.10
Fall				
Long Beach	0.43±0.11	0.40±0.08	0.36±0.07	0.45±0.10
Los Angeles	0.35±0.09	0.40±0.08	0.38±0.10	0.42±0.05

An attempt was made to determine whether average ROC or EC sizes are correlated with ROC or EC concentrations. It was concluded that if there is a dependence of size on concentration it is a very weak dependence.

Average ROC and EC size distributions are shown for the four sampling sites as functions of time of day in Figures 1 to 4. The data suggest that on some occasions (e.g., 6:00–10:00 at Long Beach) a significant amount of ROC and EC may have been associated with particles larger than the 2 μm cut for this sampling system.

CLAREMONT

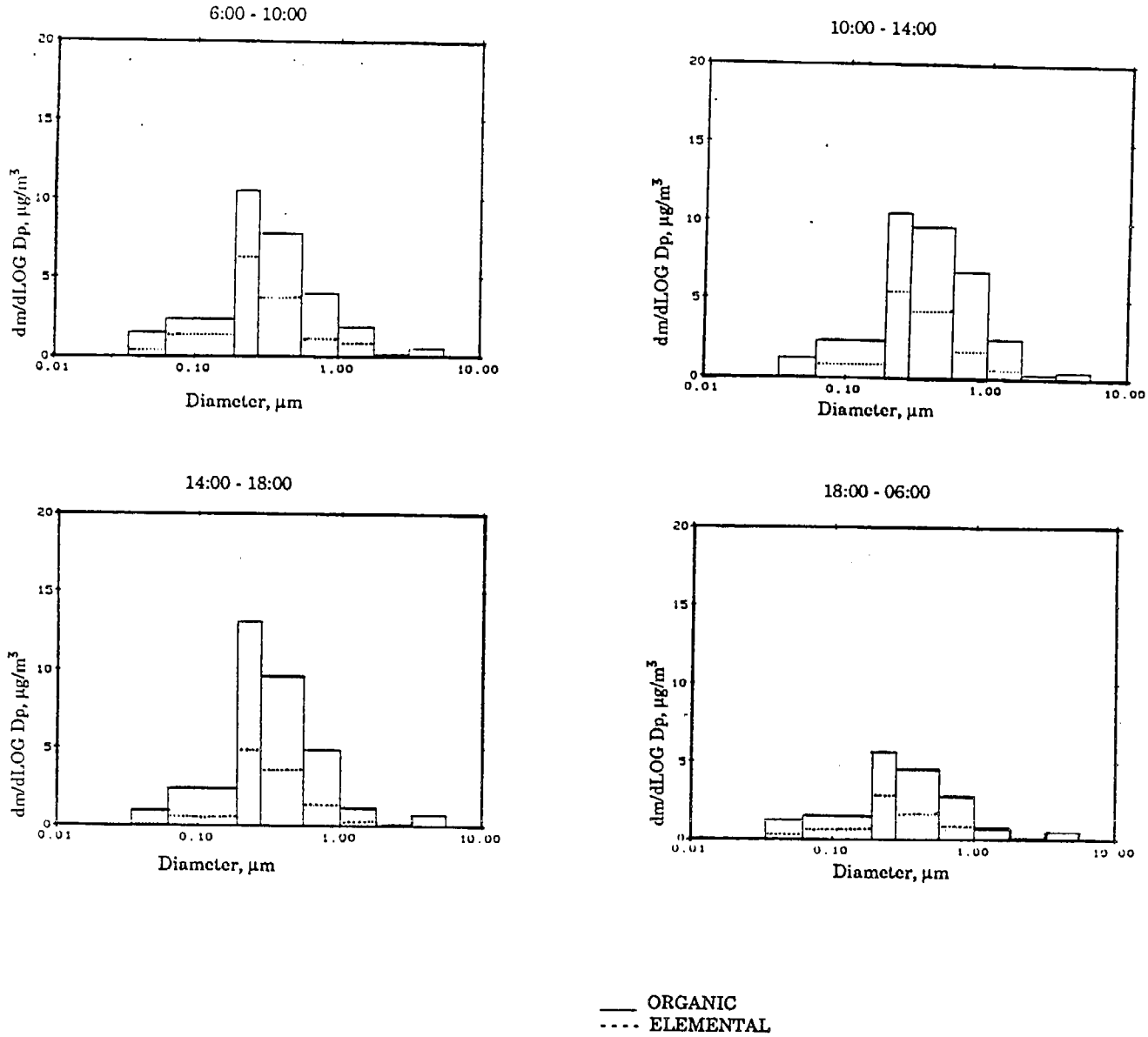

Figure 1. Average organic and elemental carbon size distributions measured at Claremont.

RUBIDOUX

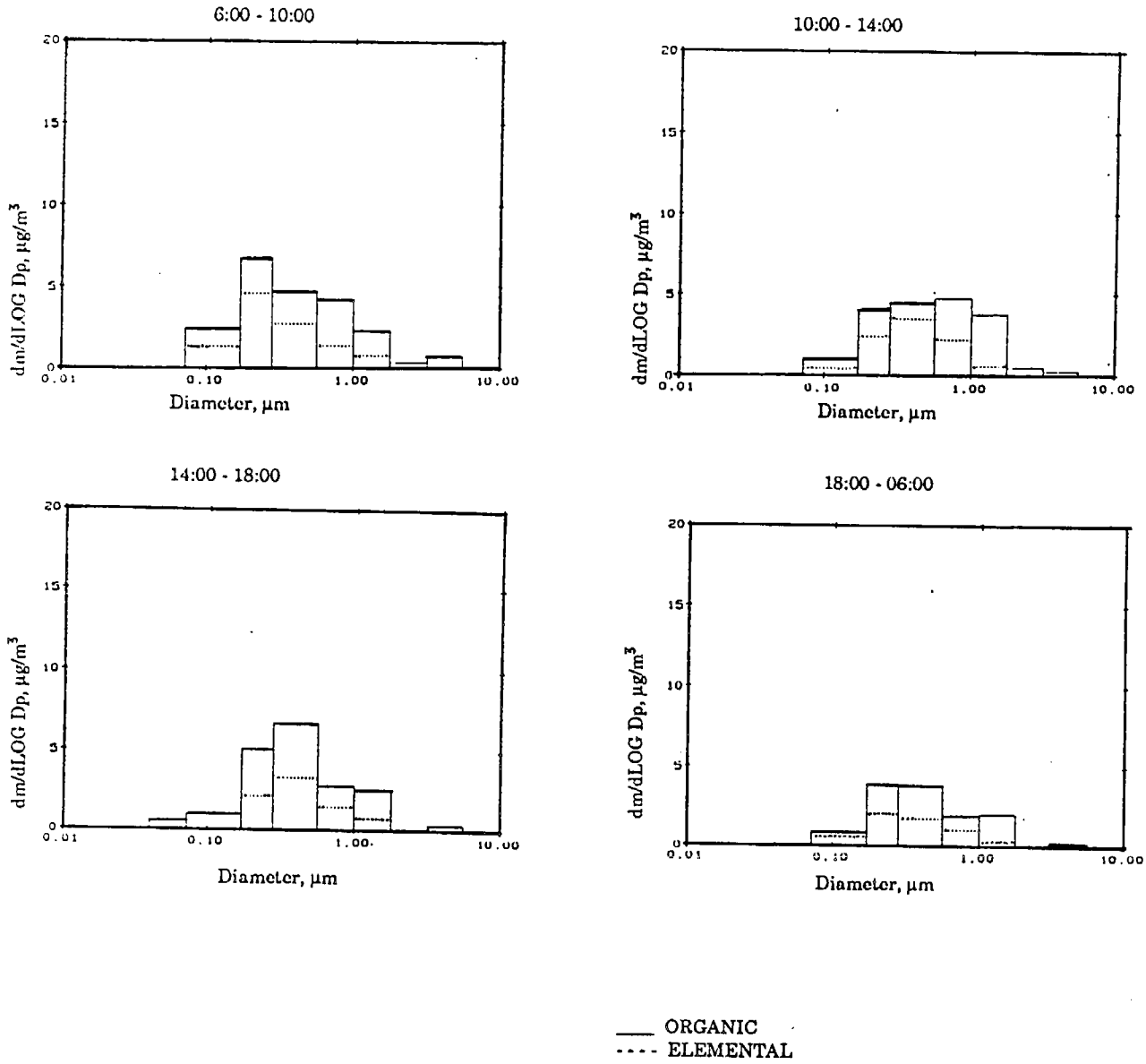

Figure 2. Average organic and elemental carbon size distributions measured at Rubidoux.

LONG BEACH

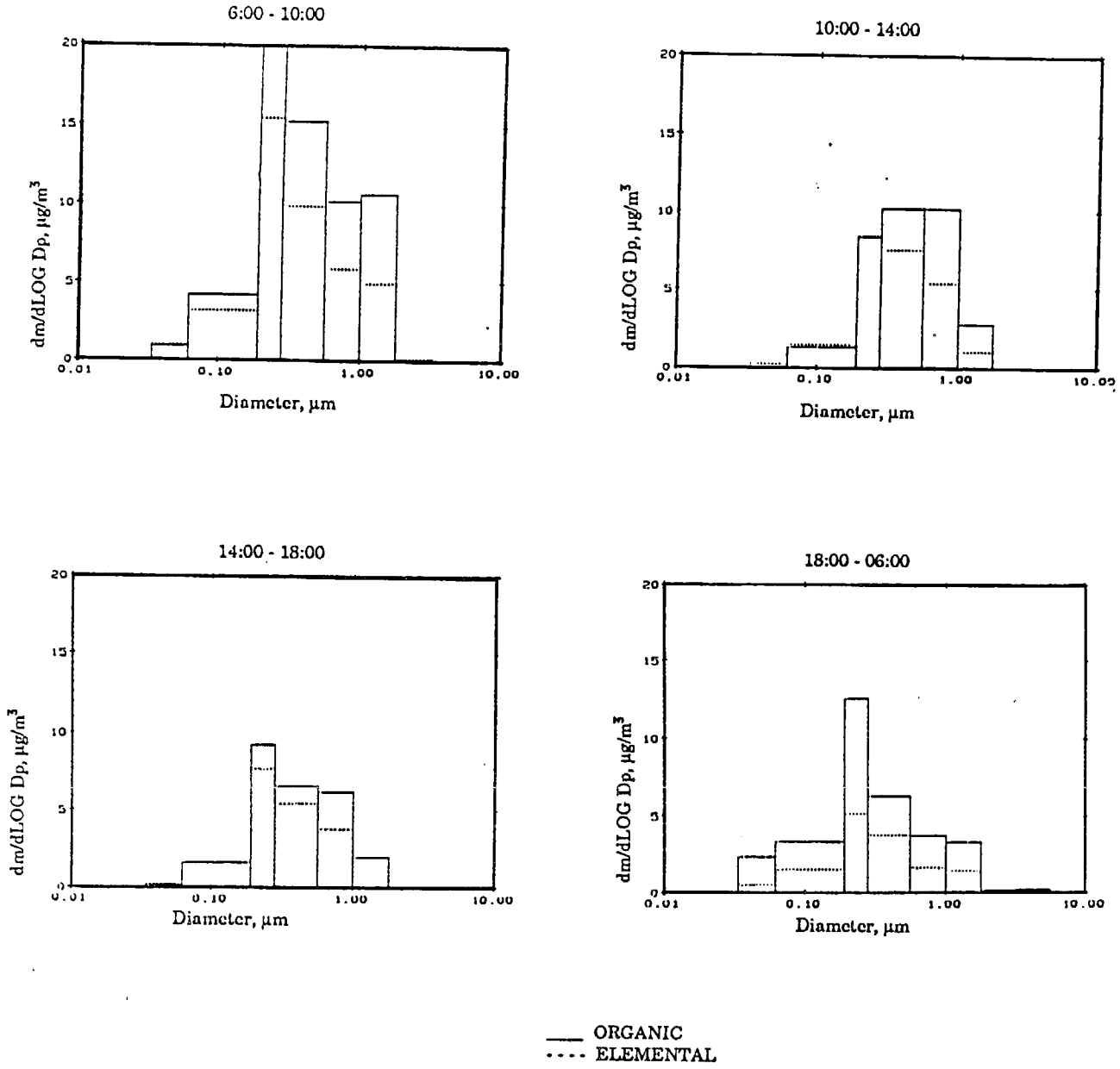

Figure 3. Average organic and elemental carbon size distributions measured at Long Beach.

LOS ANGELES

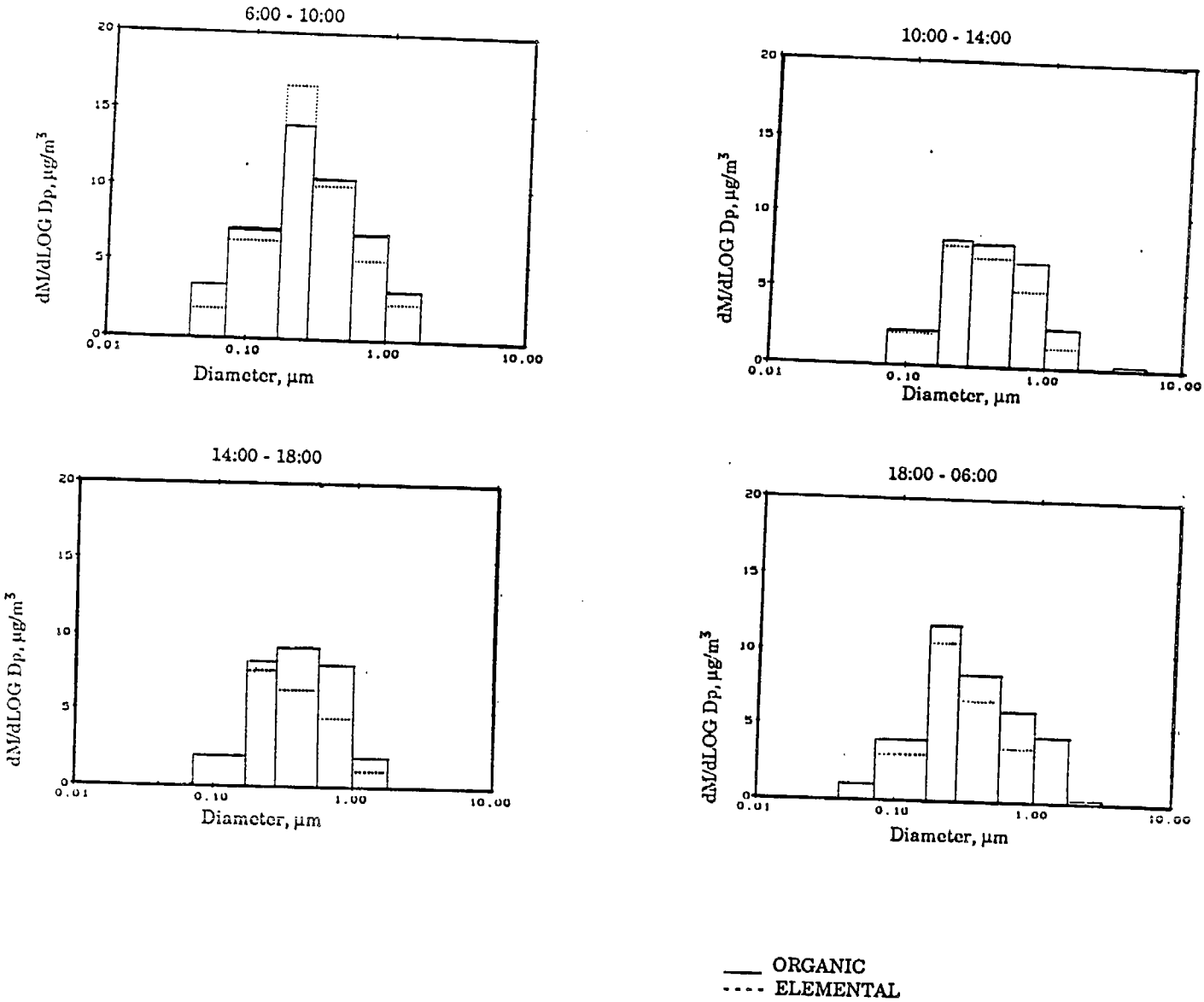

Figure 4. Average organic and elemental carbon size distributions measured at Los Angeles.

Average size–dependent ROC/EC ratios are shown as a function of particle size for each of the four sampling sites in Figures 5 to 8. The data do not show any systematic size dependence of ROC/EC ratios. For samples collected during daytime (10:00–14:00), however, there appears to be a tendency for ROC/EC to increase with increasing particle size.

Inverted Data

Examples of size distributions obtained with the Twomey and MICRON inversion algorithms are compared in Figures 9 and 10. Histograms obtained by assuming that the impactor cuts are perfectly sharp with cut points at the impactor D_{50}s are also shown. Note that there are distinct qualitative differences between results from the two inversion schemes. In particular, the MICRON results tend to be broader and less sharply peaked than the Twomey results. It should be noted that the size distribution that is returned by MICRON was found to be highly sensitive to estimated data uncertainties. The uncertainties that were used for these inversions are those discussed above in the section on blank correction and uncertainty estimates.

Size distributions are often measured with the objective of calculating some integral property. Examples of such integral properties include total mass concentration, total number concentration, optical properties (scattering, absorption or extinction coefficients), dry deposition rates, lung deposition rates, gas–particle chemical reaction rates, etc. In some cases these integral properties are proportional to integral moments of the size distribution. The mth integral moment is defined by:

$$I_m = \int_0^\infty D_p^{\,m}\, n(D_p)\, dD_p$$

where

I_m = m^{th} integral moment ($0 \le m \le 6$)
D_p = particle diameter
$n(D_p) = dN/dD_p$ = size distribution function

Note, for example, that the total mass concentration is proportional to I_3 while the total number concentration is proportional to I_0. More complex integral properties such as optical properties require integration over a more complicated function of diameter. However, it is often found that over a sufficiently narrow range of particle sizes such functions are reasonably approximated by an integral moment over that size range. With this in mind, integral moments ranging from the 0th to the 6th have been calculated for all of the Twomey and MICRON inverted MOUDI size distributions measured during SCAQS. The objective of this analysis was to determine the sensitivity of the integral moments to the data inversion method.

Comparisons of integral moments obtained with Twomey and MICRON for ROC and EC are shown in Figures 11 and 12 respectively. Note that for I_3 the agreement is quite good. This is because I_3 corresponds to total mass which was measured directly. As values of m become either larger or smaller than 3, however, the correlations between Twomey and MICRON results deteriorate. As a general rule, MICRON results are systematically greater than Twomey results for both small and large m values. Discrepancies as large as two orders of magnitude are common for I_0 or I_6.

CLAREMONT OC/EC vs Dp

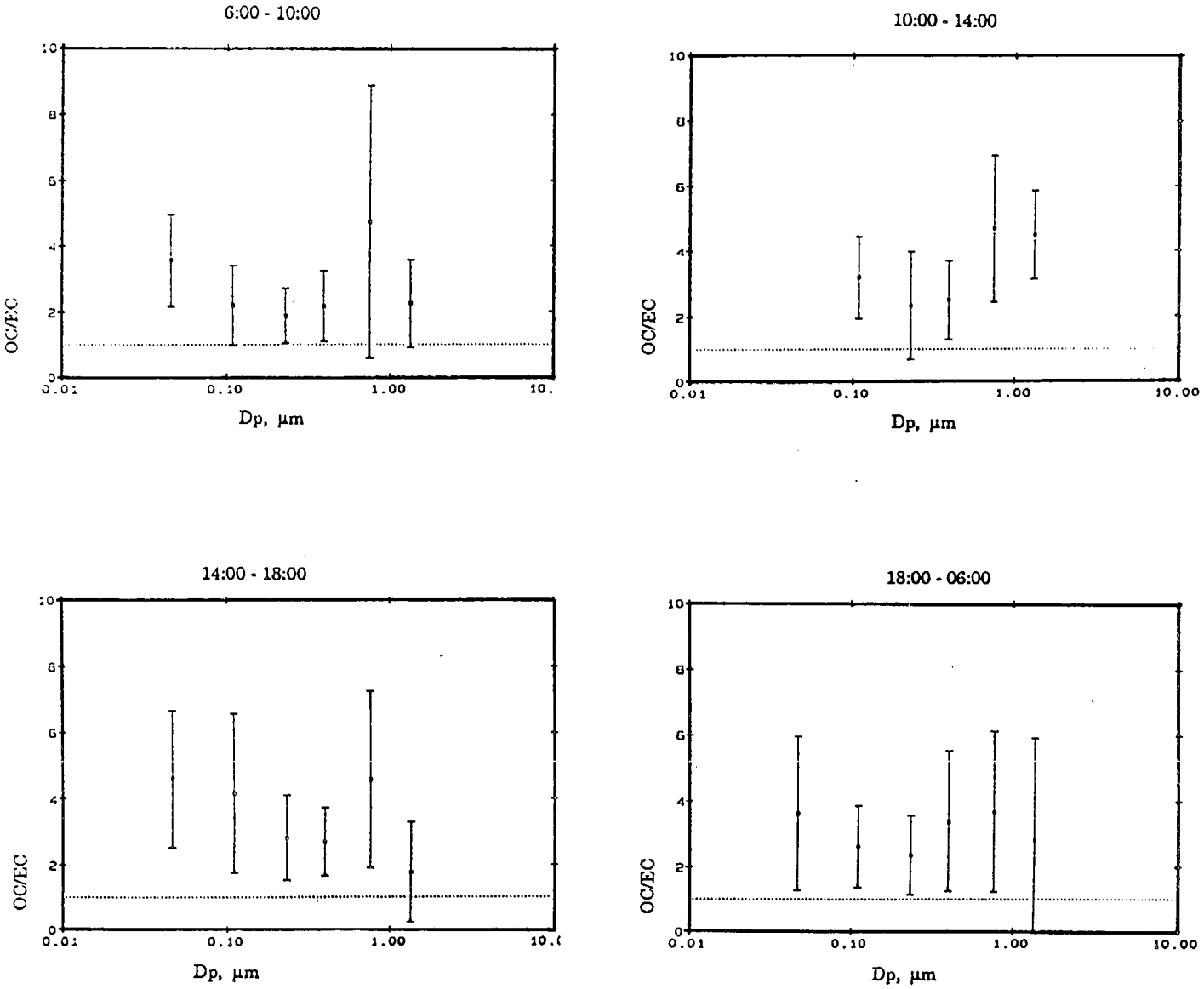

Figure 5. Average ROC/EC ratios for MOUDI data collected at Claremont as a function of particle size. Results are shown for four sampling times. The bars represent standard deviations of the means.

RUBIDOUX OC/EC vs Dp

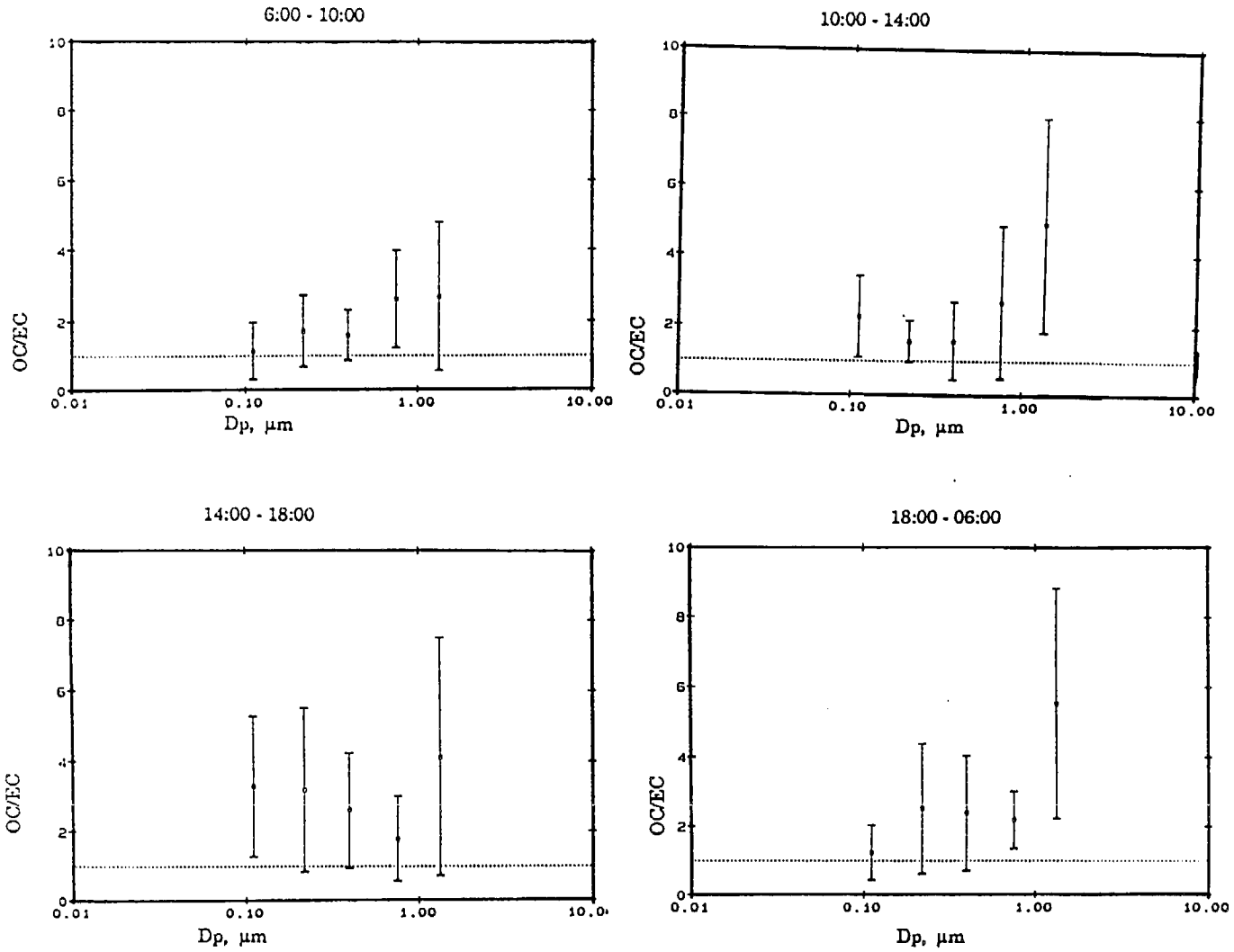

Figure 6. Average ROC/EC ratios for MOUDI data collected at Rubidoux as a function of particle size. Results are shown for four sampling times. The bars represent standard deviations of the means.

LONG BEACH OC/EC vs Dp

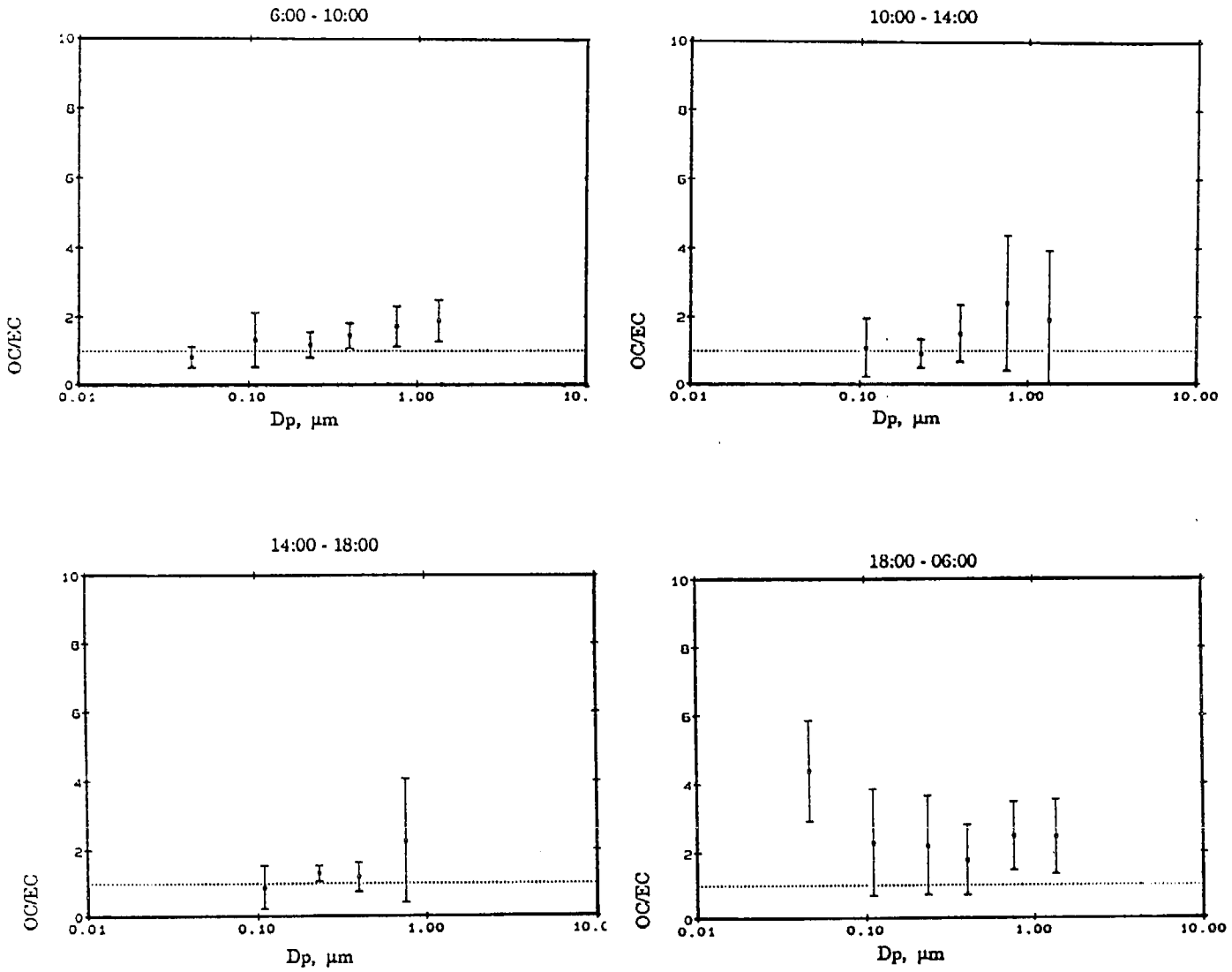

Figure 7. Average ROC/EC ratios for MOUDI data collected at Long Beach as a function of particle size. Results are shown for four sampling times. The bars represent standard deviations of the means.

LOS ANGELES OC/EC vs Dp

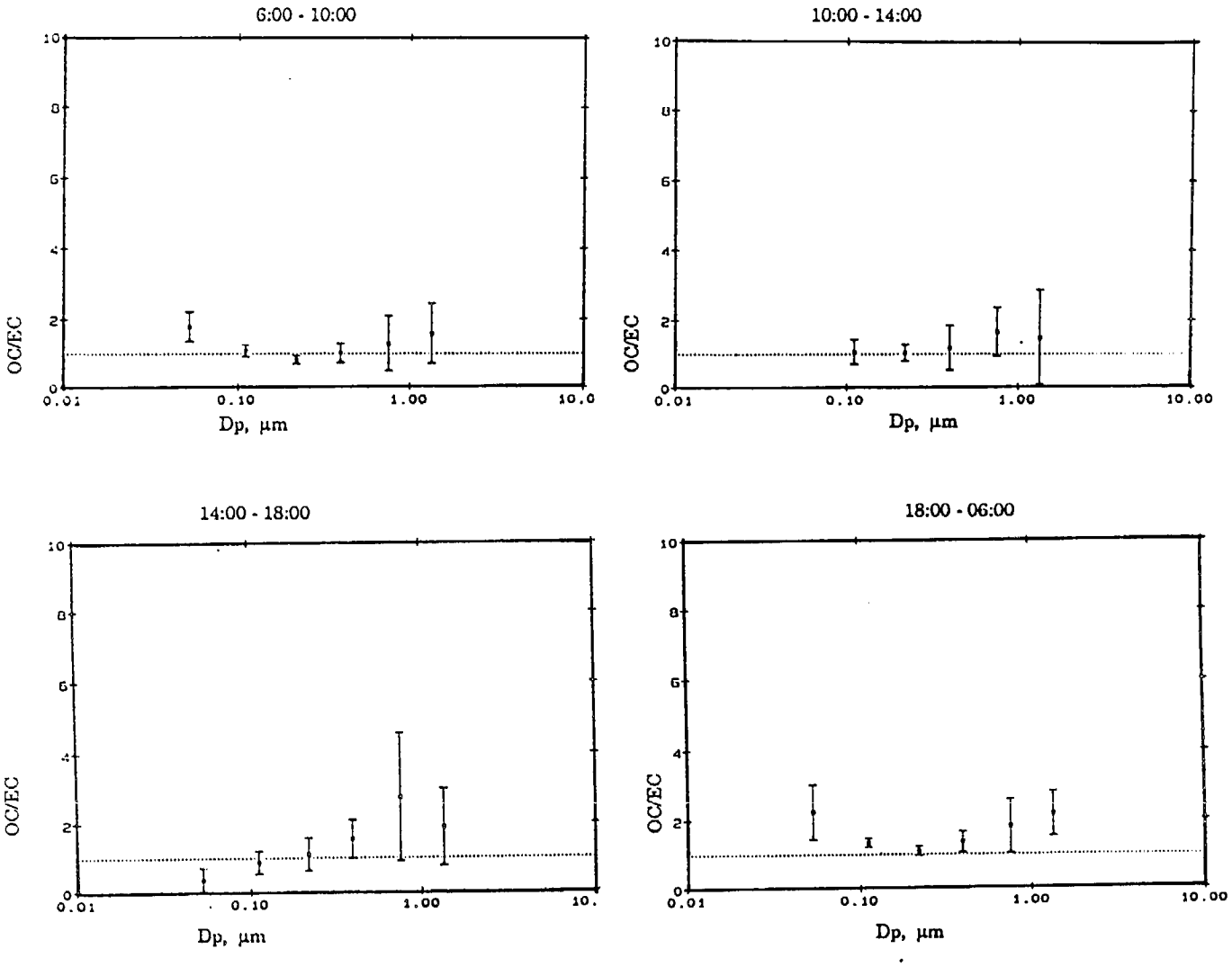

Figure 8. Average ROC/EC ratios for MOUDI data collected at Los Angeles as a function of particle size. Results are shown for four sampling times. The bars represent standard deviations of the means.

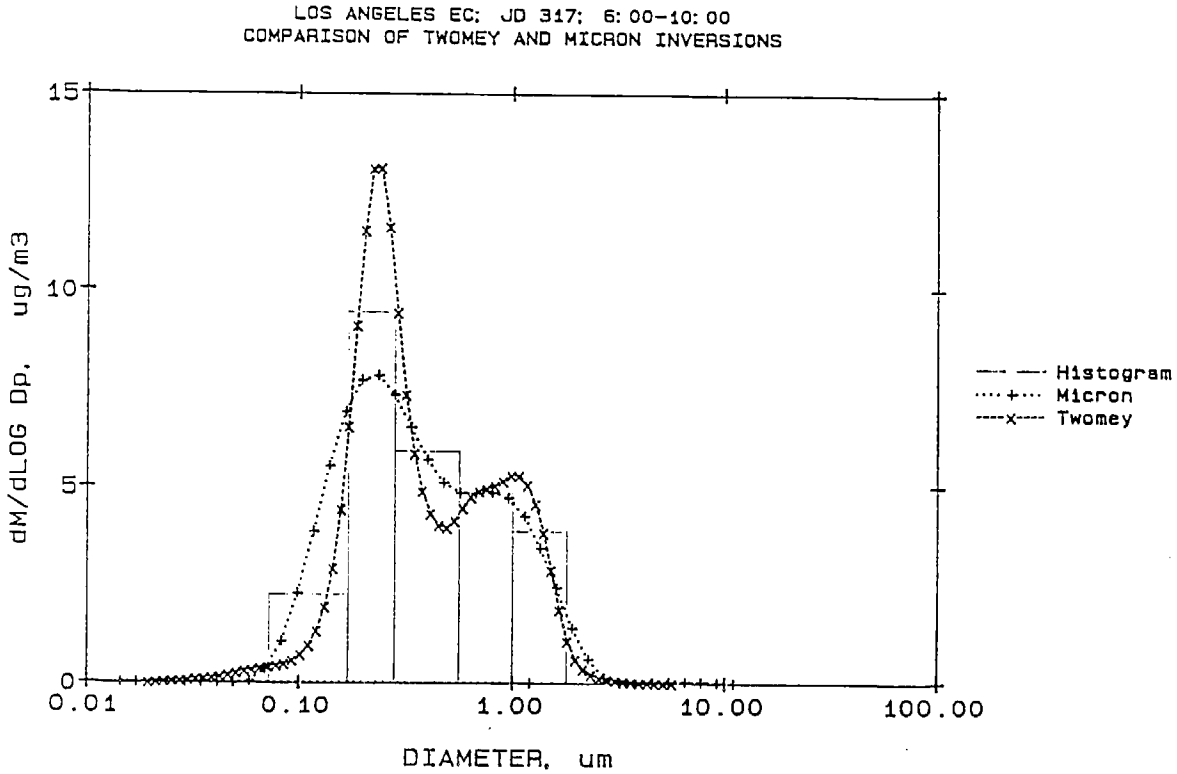

Figure 9. A comparison of raw data (histogram) with inverted size distributions obtained with the MICRON and Twomey methods.

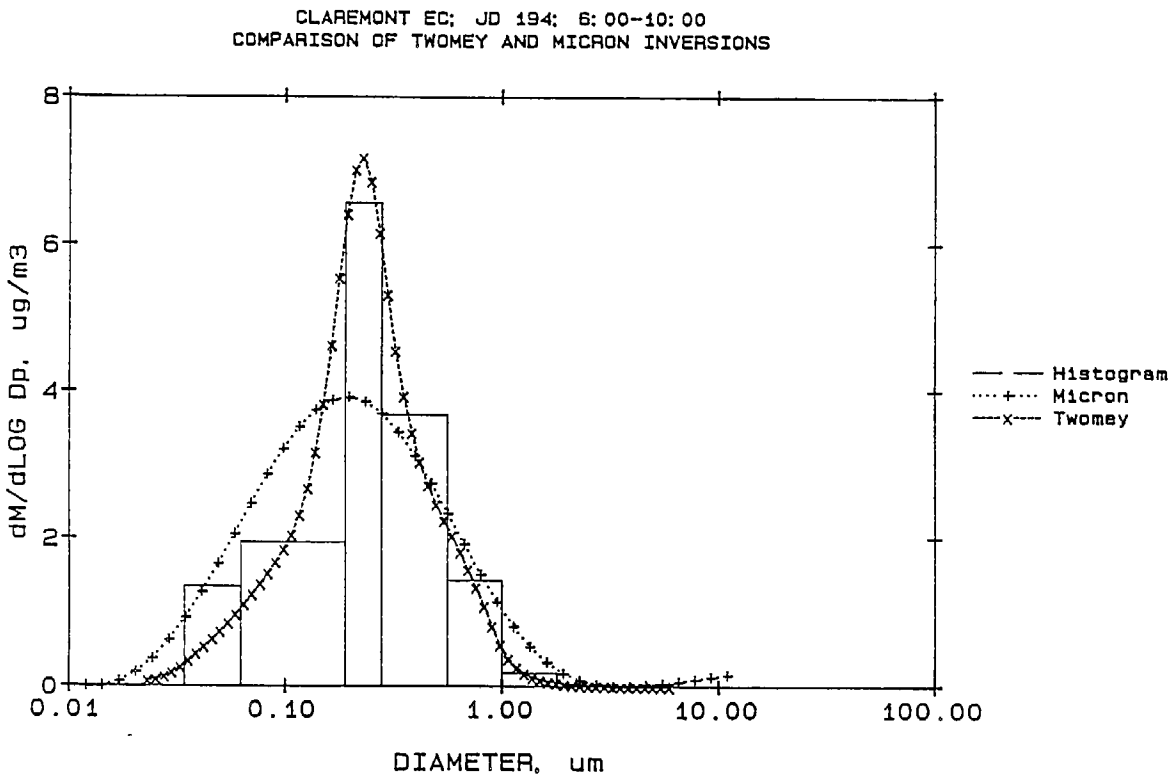

Figure 10. A comparison of raw data (histogram) with inverted size distributions obtained with the MICRON and Twomey methods.

TWOMEY vs MICRON (OC)

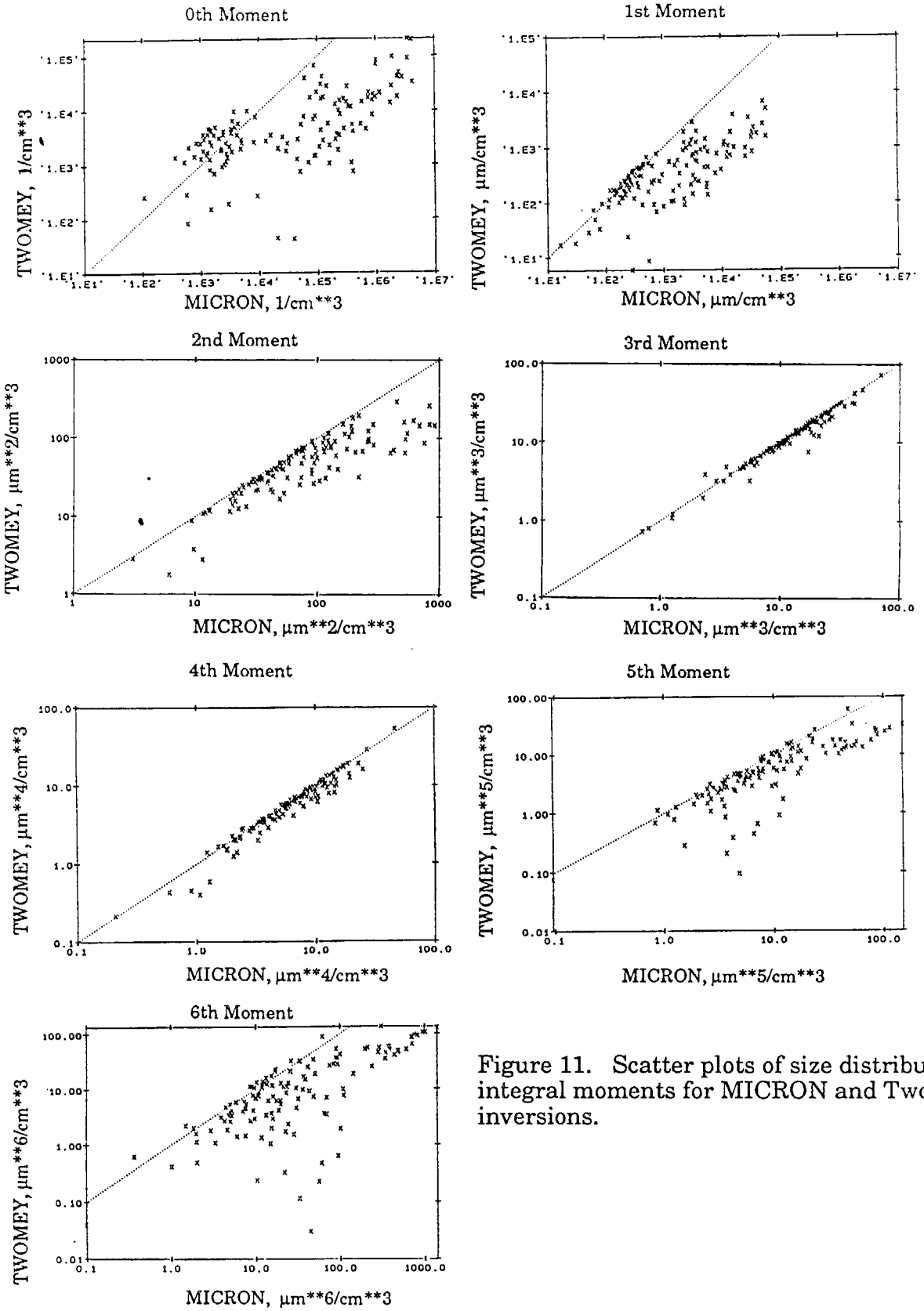

Figure 11. Scatter plots of size distribution integral moments for MICRON and Twomey inversions.

TWOMEY vs MICRON (EC)

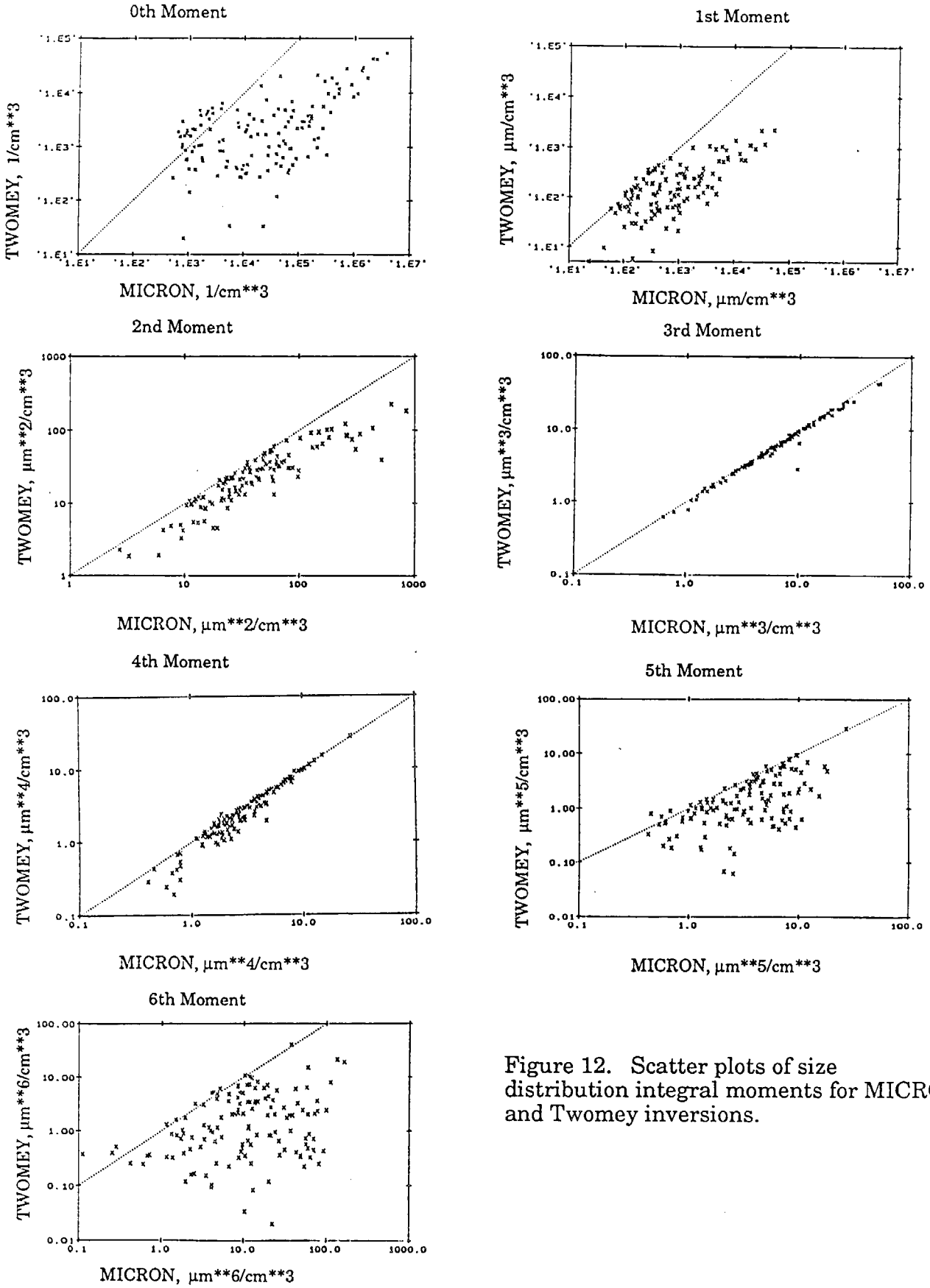

Figure 12. Scatter plots of size distribution integral moments for MICRON and Twomey inversions.

Based on the results shown in Figures 9 and 10 it is not surprising the MICRON integral moments tend to be greater than Twomey integral moments as m becomes larger or smaller than 3. Values of I_m are dominated by the small end of the mass distribution for m<3, and are dominated by the large end of the distribution for m>3. MICRON size distributions are greater than Twomey size distributions at both the small and large end of the size spectrum, and the integral moments for small or large m accentuate these differences.

The discrepancies between the Twomey and MICRON integral moments are disturbing. It is beyond the scope of this report to reach any firm conclusions regarding the validity of one or the other technique. Both methods claim to produce size distributions that are consistent with the data to within experimental uncertainties. The large discrepancies for large and small moments probably occur because they are dominated by loadings on the top and bottom impactor stages, respectively. The reported loadings on these stages were often much smaller than estimated uncertainties. Therefore, the inverted size distribution for particles that might have been caught on these stages could, in principle, vary over a wide range and still fall within uncertainty estimates. We conclude that if integral moments calculated with two different inversion methods are greatly different, then it is probably not possible to determine an accurate value for that integral with the reported data. For consistency with other SCAQS impactor measurements we have chosen to report results based on the Twomey inversion algorithm.

Winklmayr and John routinely fit multimodal lognormal distributions to the inverted size distributions. The purpose of this is to determine simple distribution parameters that can be used to characterize essential features of the size distribution, and to simplify computations involving the use of size distributions. We have used the multimodal fitting program of Winklmayr and John to fit all of the inverted MOUDI ROC and EC data. Sample comparisons of inverted size distributions and bimodal lognormal fits to the inverted size distributions are shown in Figures 13 and 14. Note that the bimodal fits are in reasonable agreement with the inverted size distributions. It was found that on average the mass of the fitted size distribution was within 3% of the mass of the measured mass.

Scatter plots showing mode mass versus mode geometric mean diameter are shown in Figures 15 to 18 for the four sampling sites. Each figure shows results for a given site. The results on the top of the figures apply to the Twomey inversions while the results on the bottom apply to MICRON. The two figures on the left side of each page are for ROC and the two on the right are for EC. The most striking result is in these figures is in Figure 18. Note that Twomey shows both ROC and EC to be separated into two modal groups. Modal separations from MICRON are not so distinct.

Frequency distributions for mode geometric mean diameters are shown in Figures 19 and 20. Again, results are given for both the Twomey (top) and MICRON (bottom) inversions. Each distribution contains results for ROC and EC. Figure 19 applies to Claremont and Rubidoux data, and Figure 20 applies to Long Beach and Los Angeles data. Note that bimodal fits to Twomey inversions are more likely to produce a mode at the large particle end (near 1 μm) of the size spectrum. Note also that there is typically a rather close correlation between modal frequencies for ROC and EC.

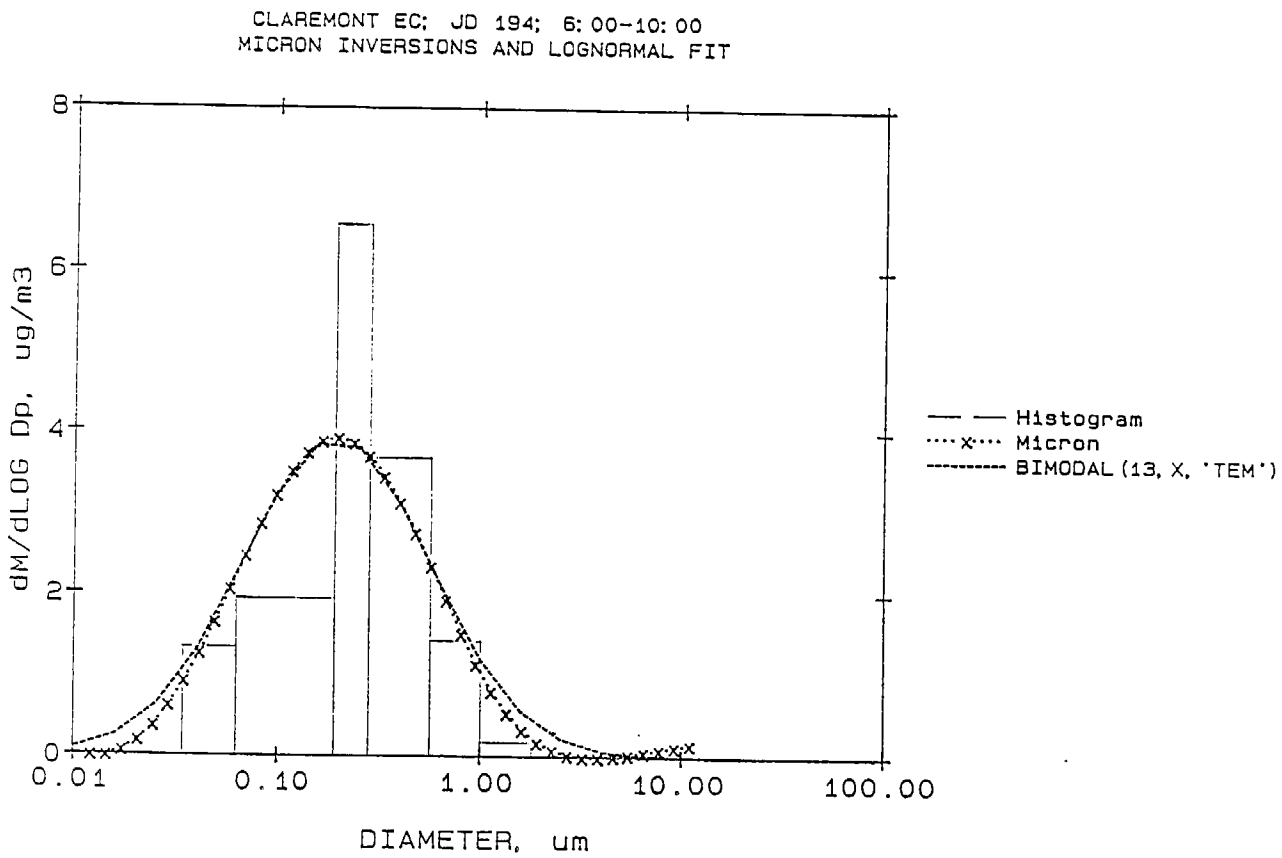

Figure 13. Comparison of raw data (histogram), MICRON inverted size distribution, and lognormal fit to the MICRON inverted size distribution.

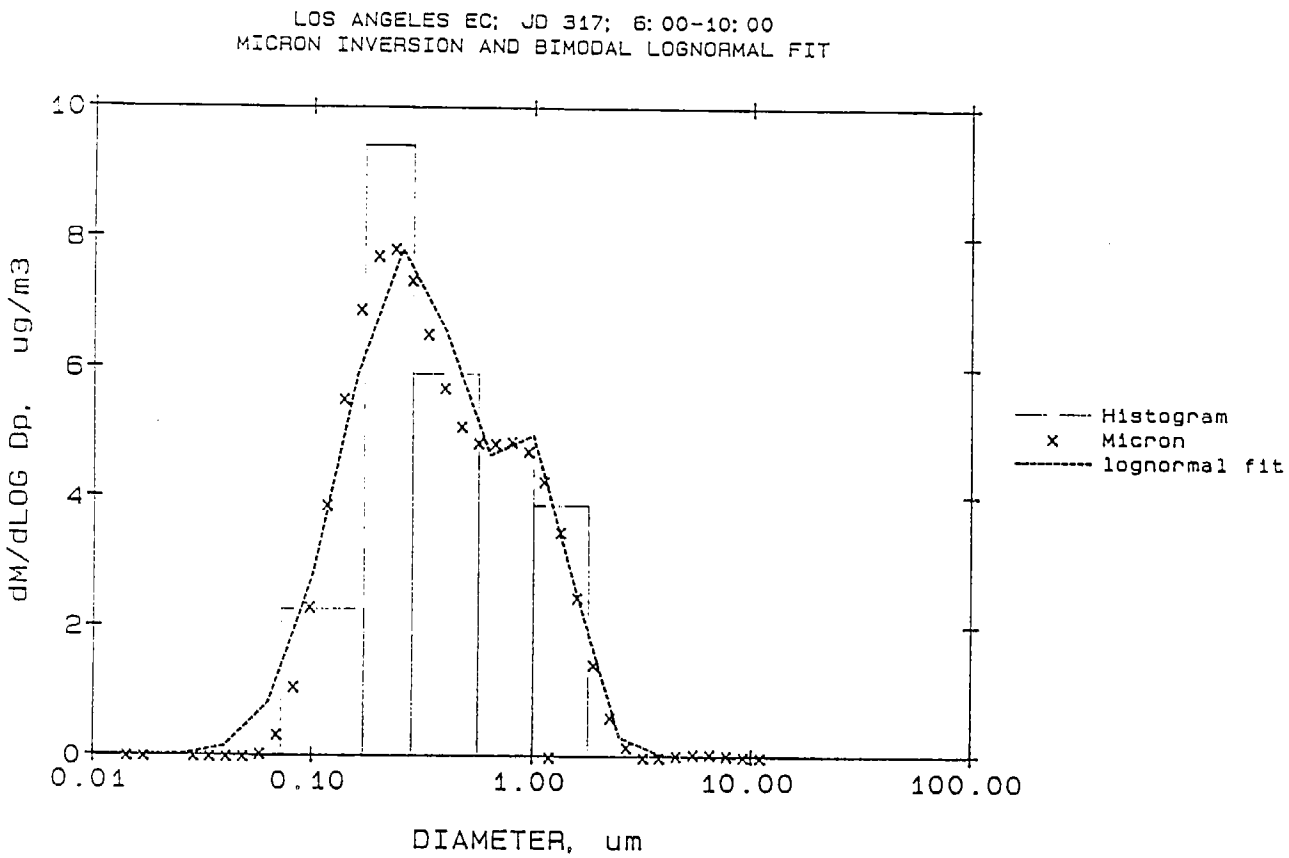

Figure 14. Comparison of raw data (histogram), MICRON inverted size distribution, and lognormal fit to the MICRON inverted size distribution.

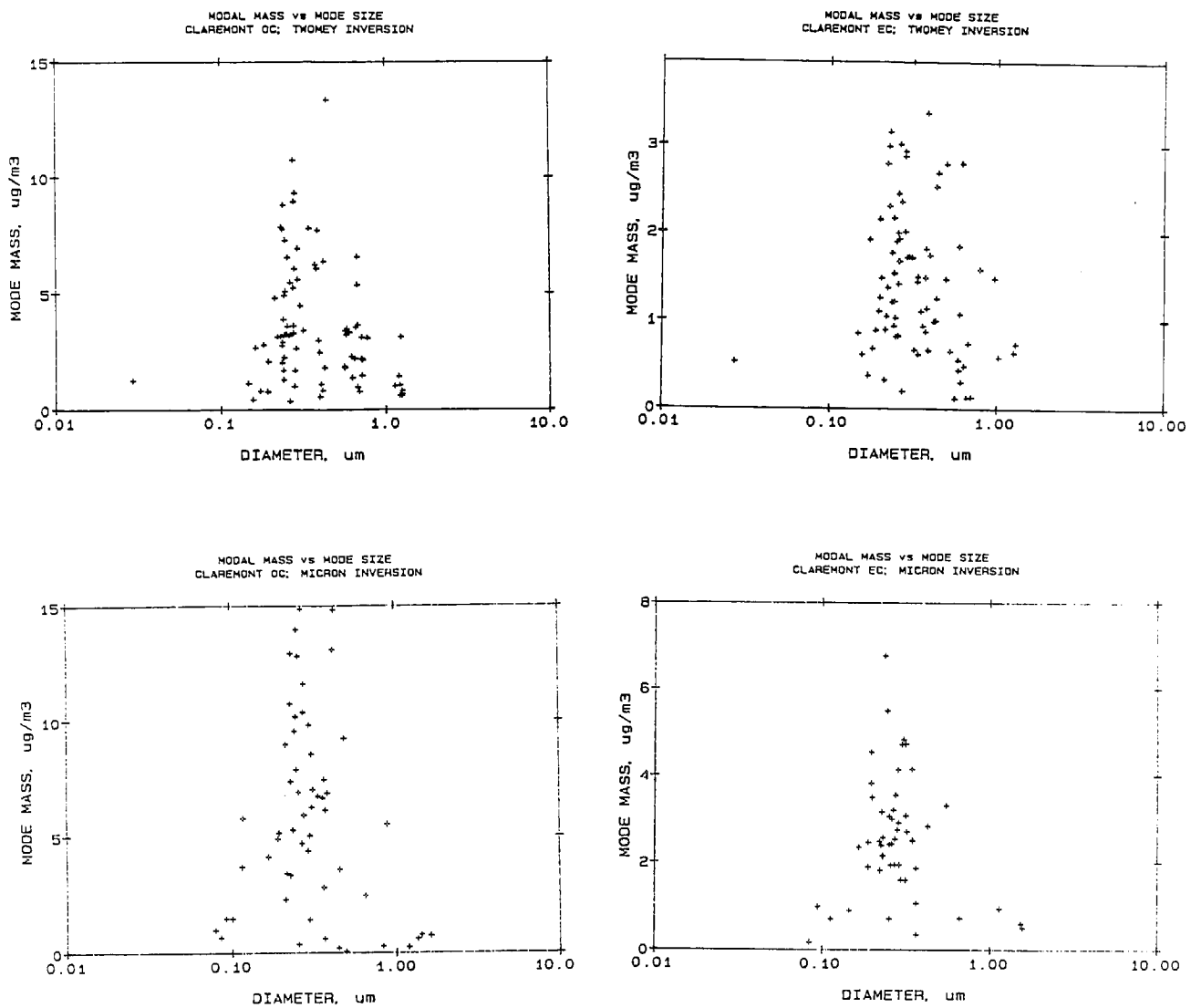

Figure 15. Modal mass versus geometric mean diameter for Claremont ROC and EC data. The results on the top of the page were obtained with the TWOMEY inversion while the results on the bottom were obtained with MICRON.

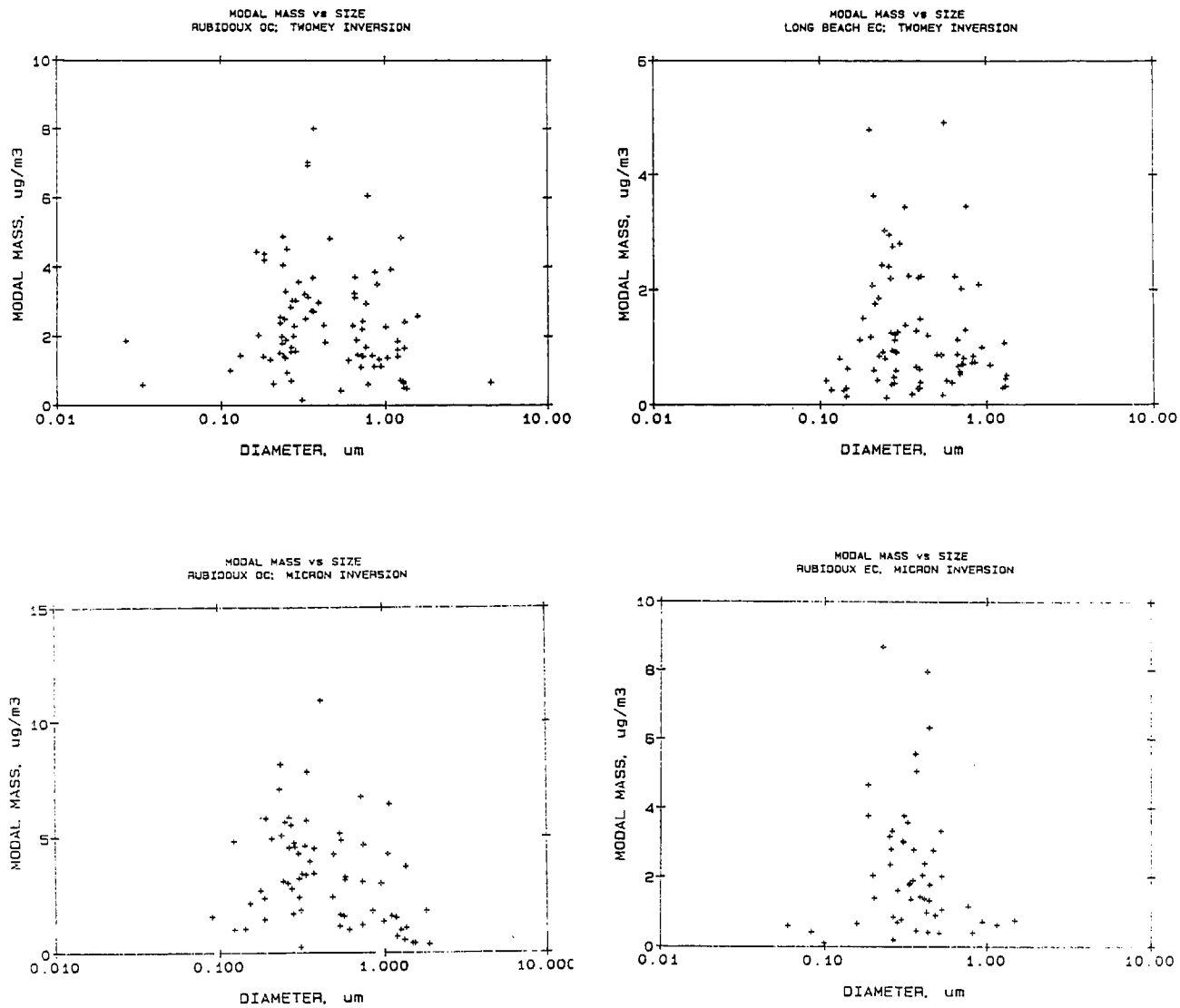

Figure 16. Modal mass versus geometric mean diameter for Rubidoux ROC and EC data. The results on the top of the page were obtained with the Twomey inversion while the results on the bottom were obtained with MICRON.

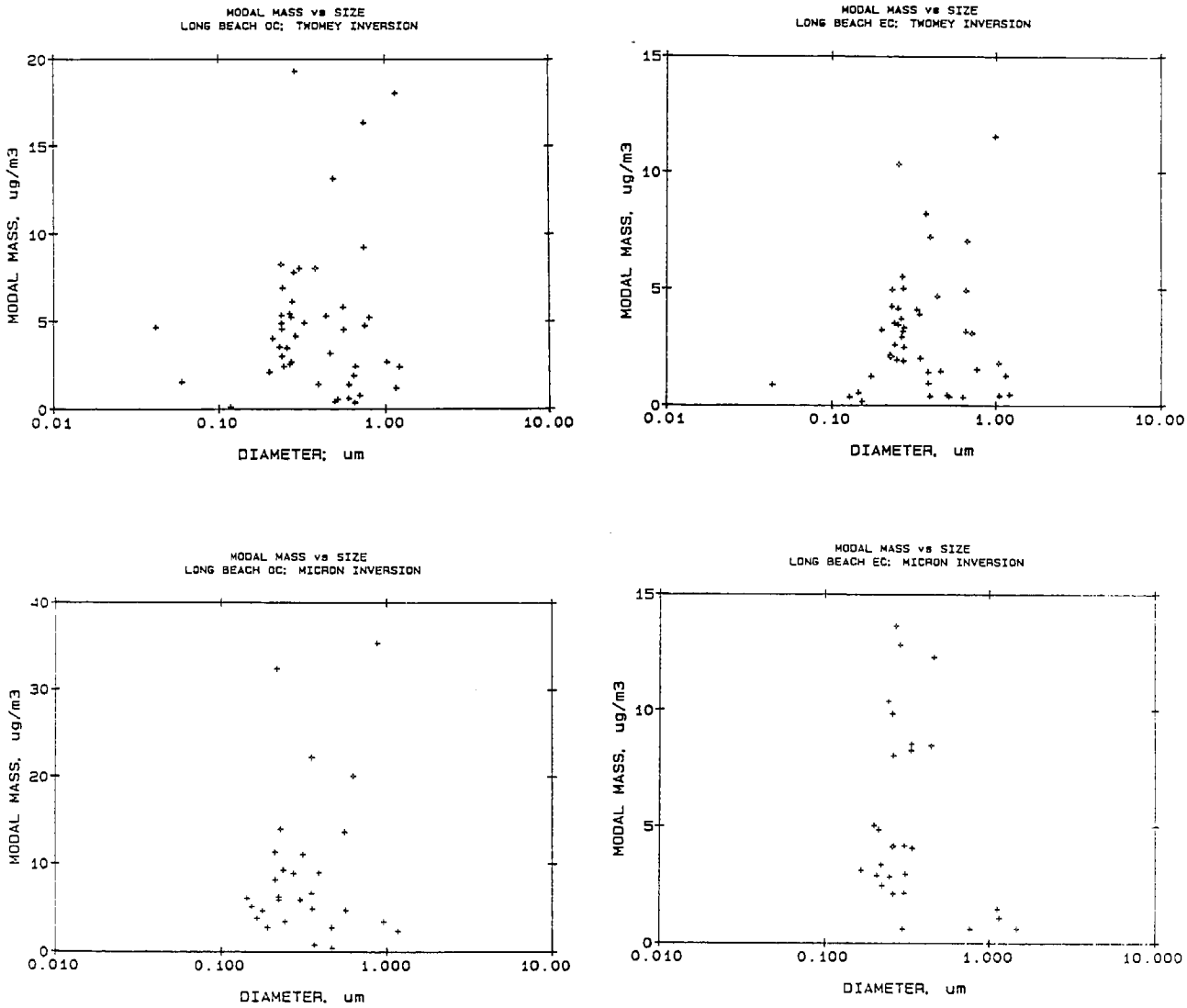

Figure 17. Modal mass versus geometric mean diameter for Long Beach ROC and EC data. The results on the top of the page were obtained with the Twomey inversion while the results on the bottom were obtained with MICRON.

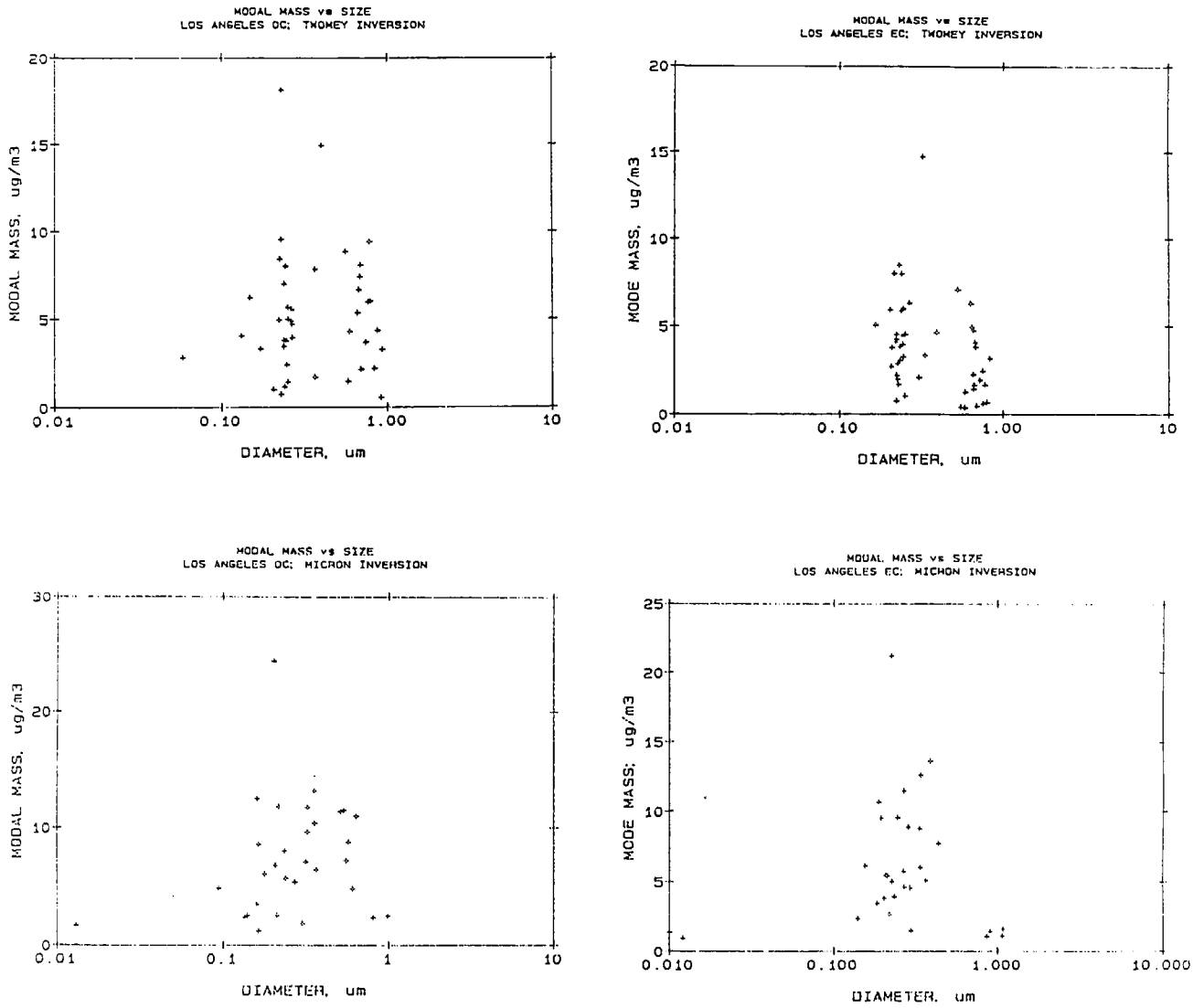

Figure 18. Modal mass versus geometric mean diameter for Los Angeles ROC and EC data. The results on the top of the page were obtained with the Twomey inversion while the results on the bottom were obtained with MICRON.

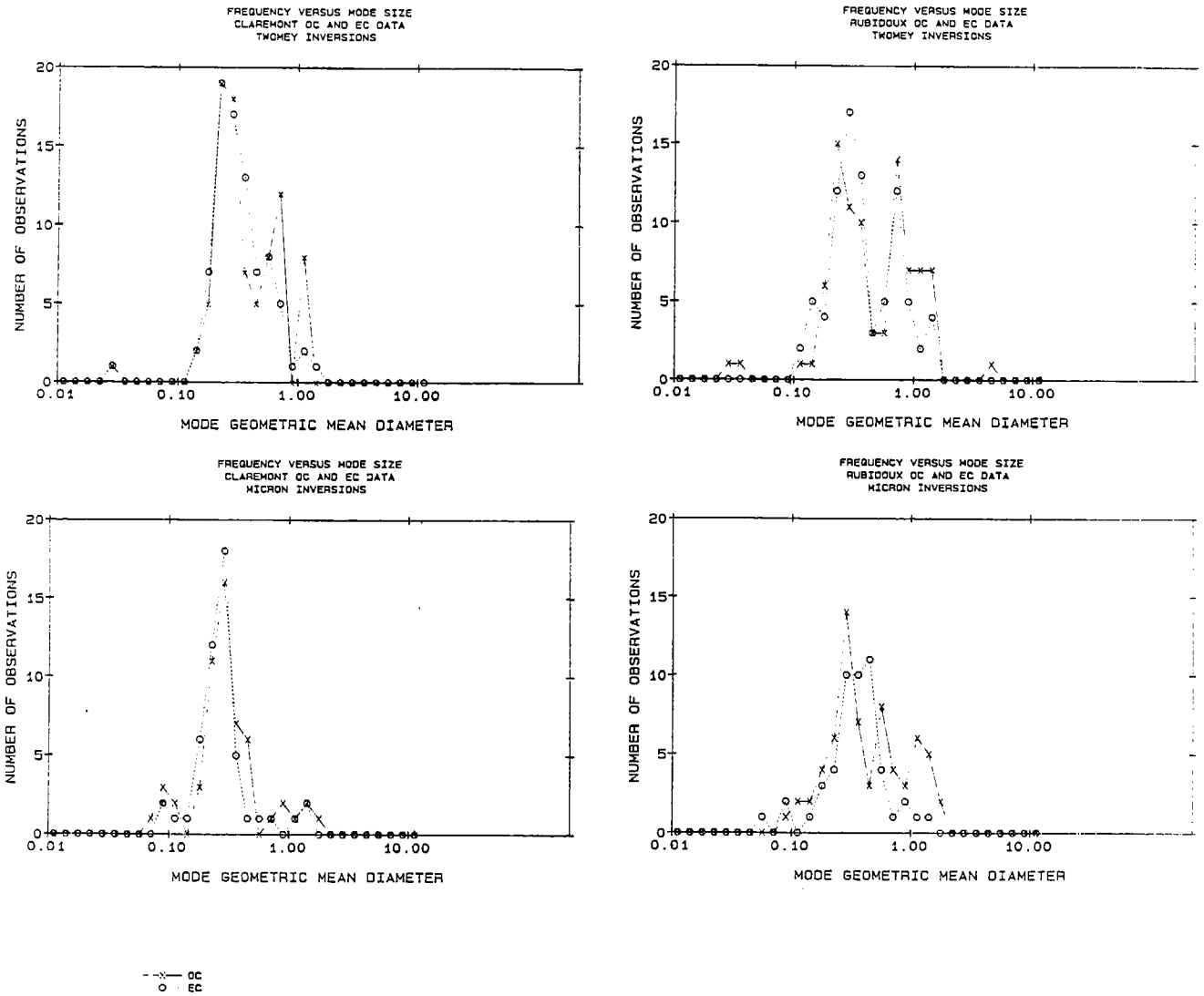

Figure 19. Frequency distributions for Claremont and Rubidoux modal geometric mean diameters for ROC and EC. Results are shown for both Twomey (top) and MICRON (bottom) inversions.

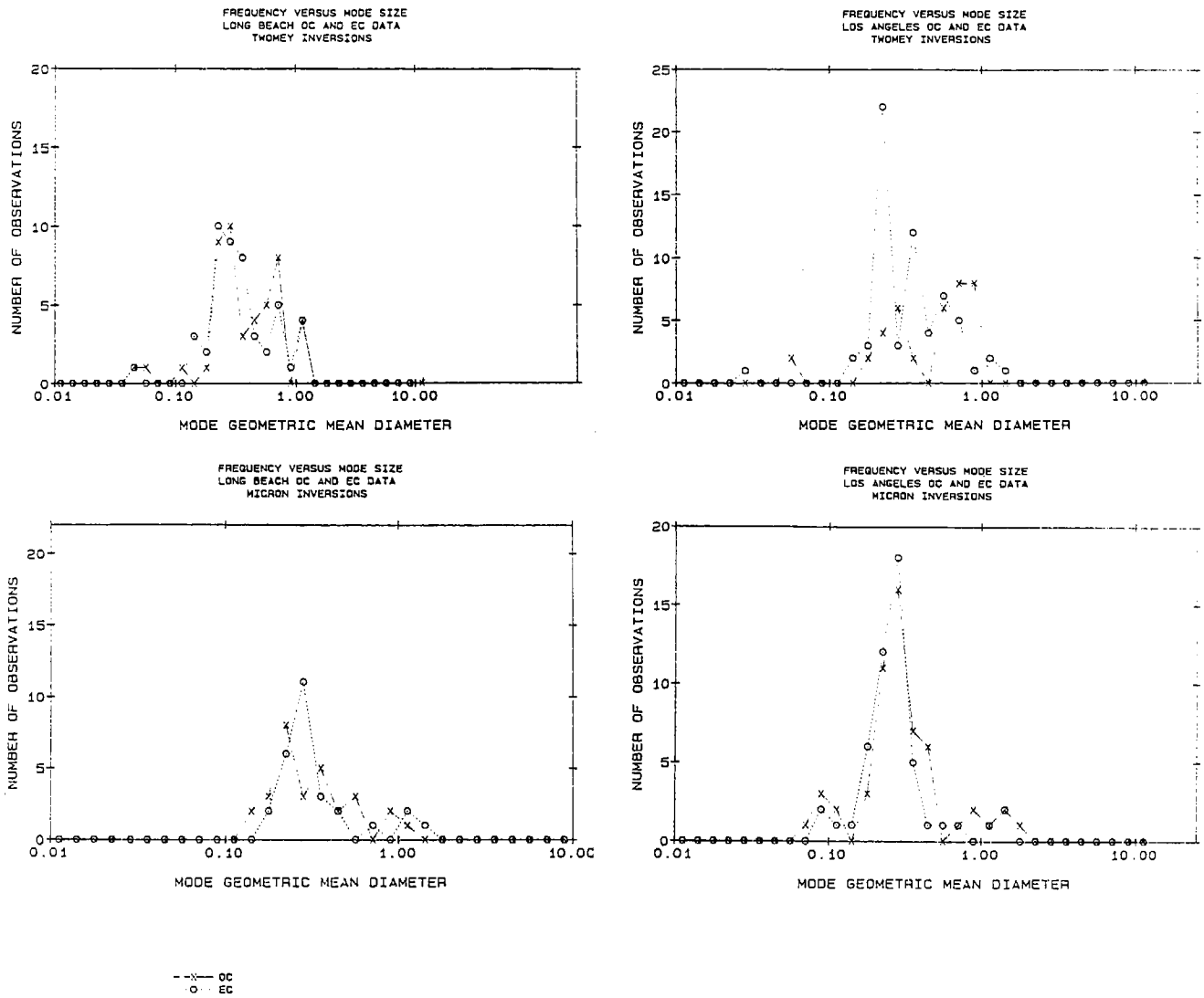

Figure 20. Frequency distributions for Long Beach and Los Angeles modal geometric mean diameters for ROC and EC. Results are shown for both Twomey (top) and MICRON (bottom) inversions.

Comparison With Data From Other Carbon Samplers

MOUDI ROC and EC data from Claremont have been compared with similar data from other samplers. Results of those comparisons are discussed in this section. The total ROC and EC concentrations from MOUDI samples were obtained by adding the loadings on all stages excluding the afterfilters. The afterfilters were excluded because of adsorption artifacts that have been encountered in previous work (McMurry and Zhang, 1989). Excluding the afterfilter data should have a minor effect on the total ROC or EC loadings since only a small fraction of the total fine particle loading is likely to be found in particles too small to be collected on the bottom impactor stage (≃0.05 μm cutoff diameter).

C with ROC collected with the SCAQS sampler are shown in Figures 21 to 23. Quartz filters were used to collect fine (sub–2.5 μm) samples for ROC and EC analyses. Samples were also collected on a quartz filter located downstream of a Teflon prefilter. The purpose of the quartz backup filter was to correct for artifacts due to gas adsorption. Analyses of filters collected with the SCAQS sampler were also done at ERT using the same technique that was used for the MOUDI samples.

In Figure 21 the SCAQS filter ROC loadings without adsorption correction are plotted against the MOUDI data (stages plus afterfilter). Note that the SCAQS filter data were systematically higher than the MOUDI data, but that the slope of the correlation (1.11) is reasonably good. McMurry and Zhang (3) present arguments to show that organic vapor adsorption can lead to substantially inflated ROC measurements on quartz filters such as those used in the SCAQS sampler. Based on these arguments it is believed that the SCAQS filter data in Figure 21 which are not corrected for adsorption probably overestimate the true ROC loadings.

In Figure 22 the adsorption–corrected SCAQS sampler fine particle ROC (filter minus afterfilter) are compared with MOUDI ROC (sum of stages excluding afterfilter). This plot provides our best estimate of the true ROC concentrations obtained with the SCAQS sampler and the MOUDI. Again, the SCAQS sampler is systematically higher than the MOUDI, and the correlation coefficient is poorer than for the data shown in Figure 21, where no adsorption correction was made.

Fine particle EC concentrations measured with the SCAQS sampler and the MOUDI are shown in Figure 23. Again, correlations are poor. MOUDI EC concentrations typically exceed Filter EC concentrations. This is in contrast to the ROC data where the filter concentrations are mostly higher.

MOUDI EC data are compared with data from the photoacoustic spectrometer operated by Ford (6) in Figure 24. Unlike the MOUDI method, the photoacoustic technique is based on insitu measurements of optical absorption. Although the MOUDI EC values are typically lower than the spectrometer, this correlation is better than the filter–MOUDI correlation. This is a surprising result given the different measurement principles. A similar result was found for data from the 1986 Carbonceous Species Methods Comparison Study (5) the where the best correlation for MOUDI EC data was with the LBL aethalometer (7), another optical absorption device.

The poor quality of the correlations between ROC and EC loadings for measurements with different samplers was expected based on previous experience (5). Reasons for these poor correlations are not understood. It is likely that both sampling and analytical methods play a significant role.

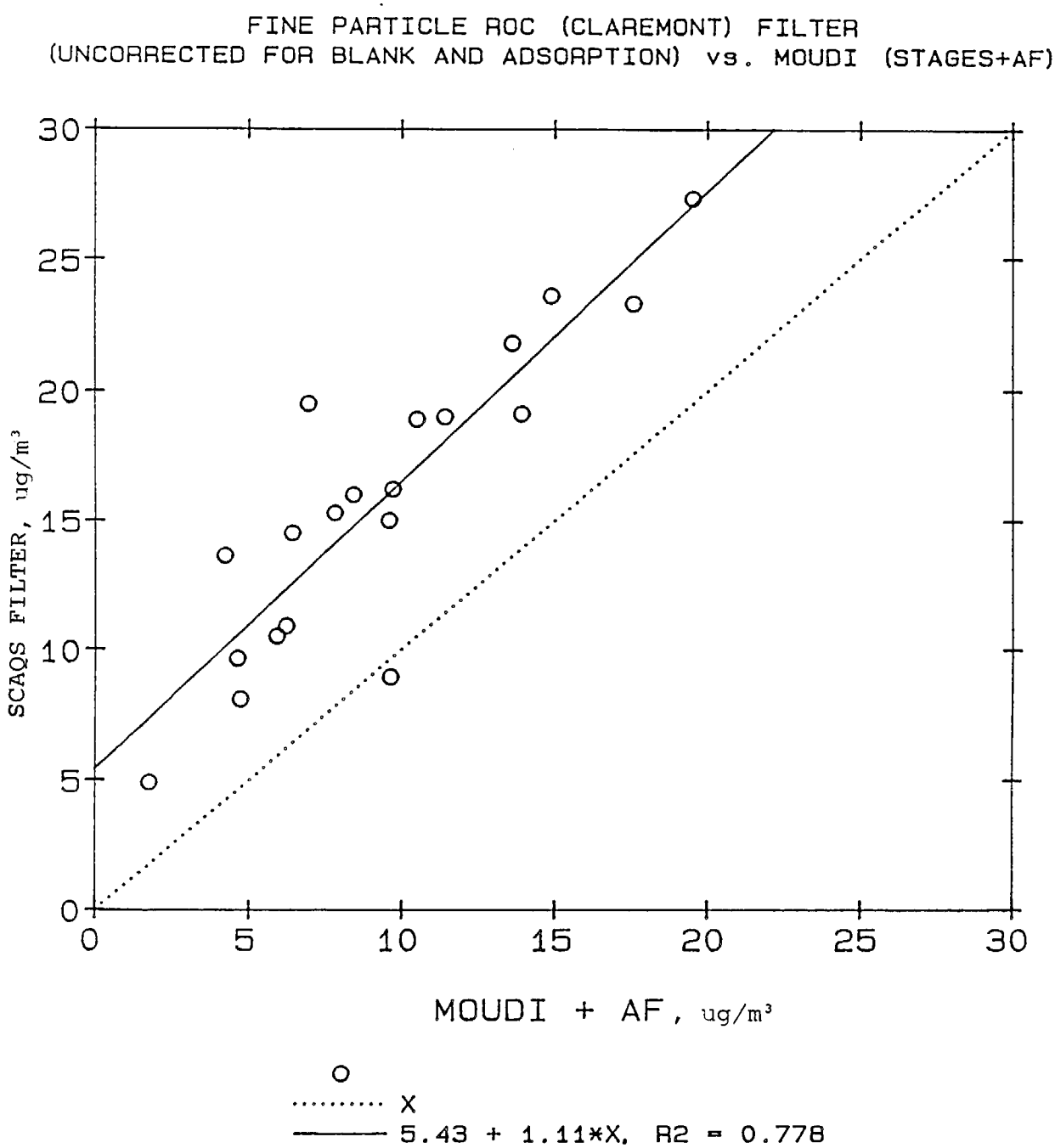

Figure 21. Fine particle ROC collected with the SCAQS sampler versus the MOUDI. No blank correction was done for the SCAQS sampler. The MOUDI data were obained by adding loadings from all stages plus the afterfilter.

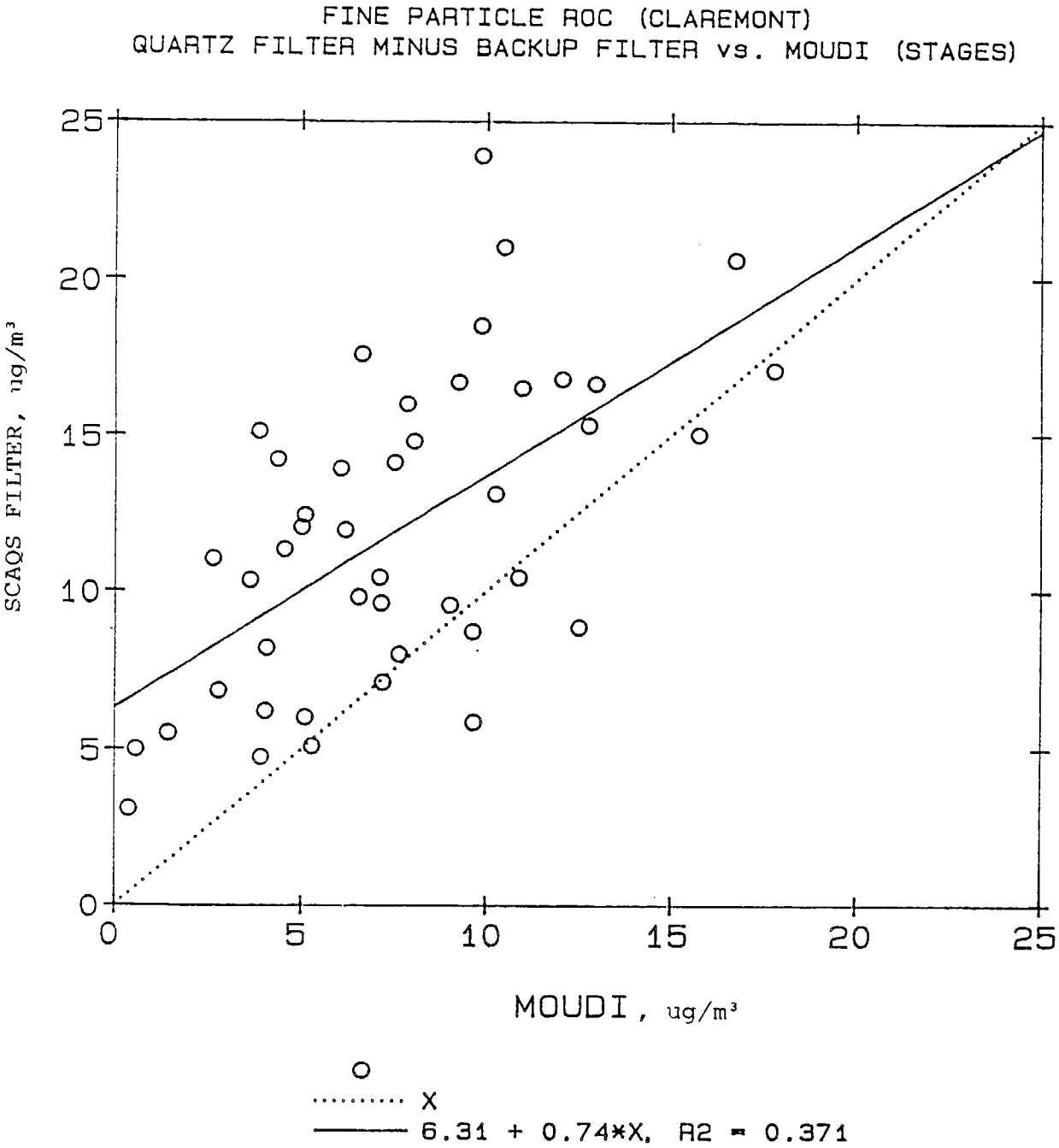

Figure 22. Fine particle ROC collected with the SCAQS sampler versus the MOUDI. The SCAQS sampler data have been corrected for blank and adsorption by subtracting the loading from a quartz filter located downstream of a Teflon filter. The MOUDI data were obtained by adding loadings from all stages (excluding the afterfilter). The amount of particulate ROC on the MOUDI afterfilter should be negligible since the lower size cuts of the bottom stages are about 0.05 um.

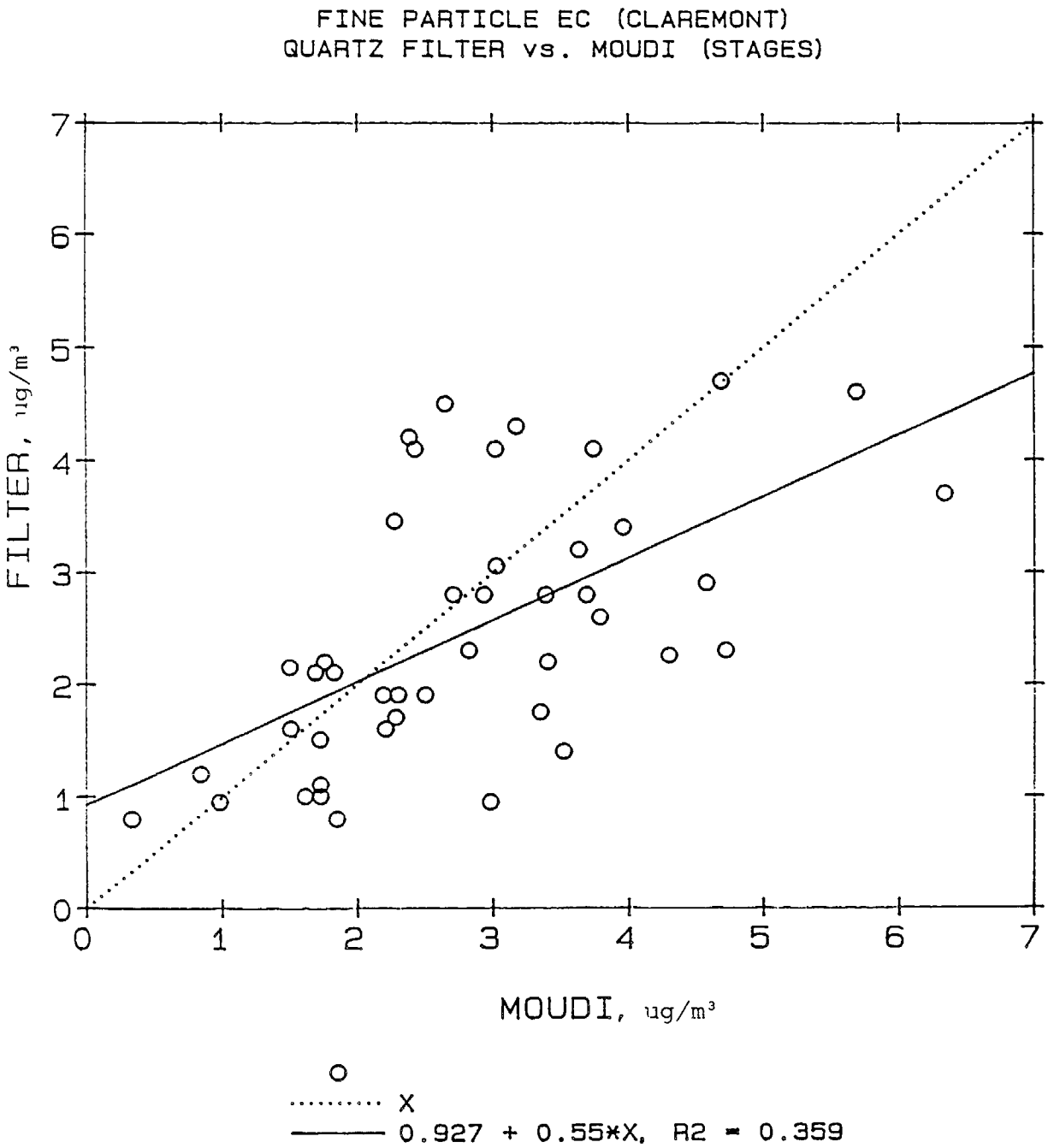

Figure 23. Fine particle EC collected with the SCAQS sampler versus the MOUDI.

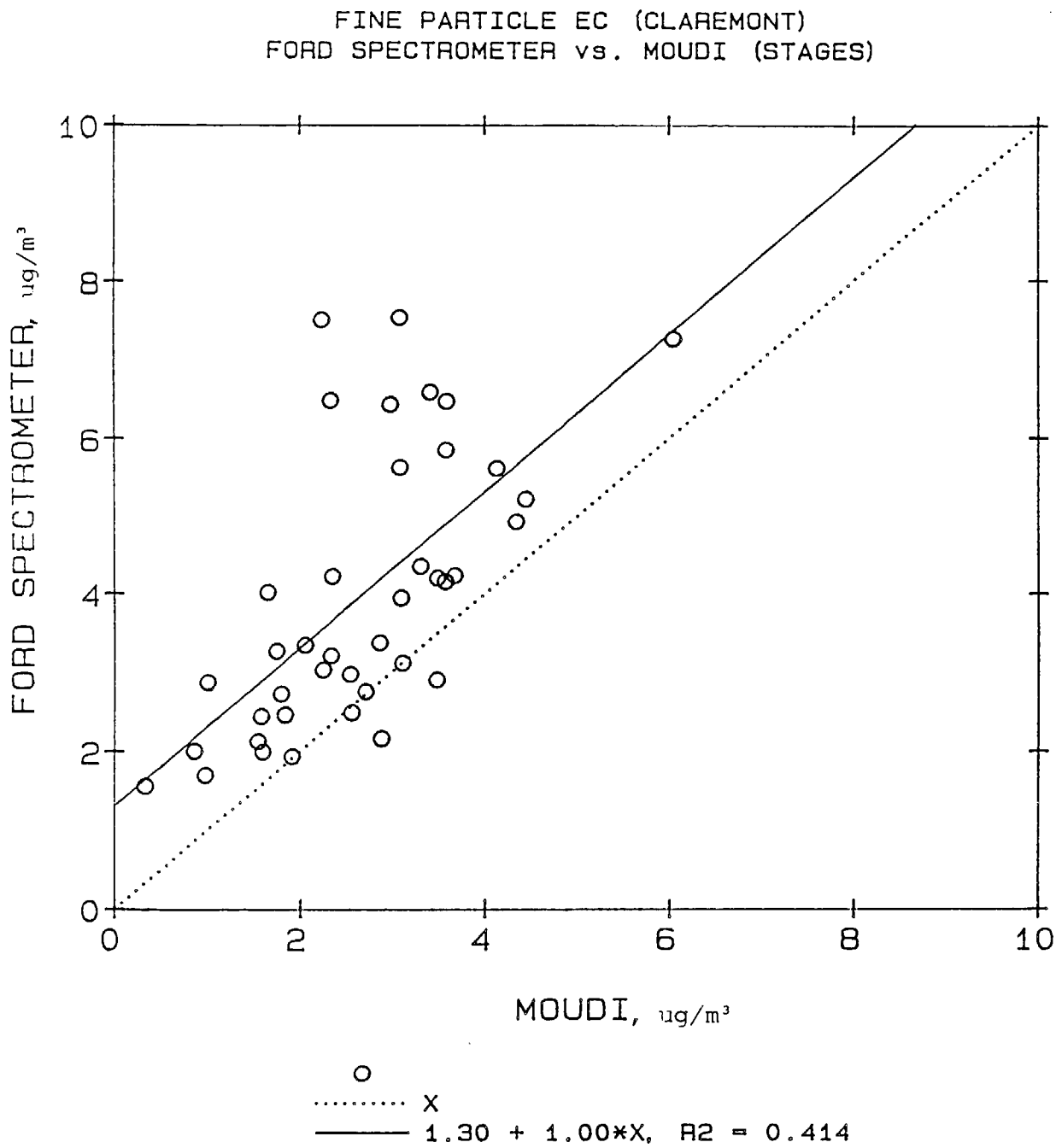

Figure 24. Fine particle EC collected with the Ford spectrometer versus the MOUDI.

ACKNOWLEDGMENTS

This research was supported primarily by the Coordinating Research Council, 219 Perimeter Center Parkway, Atlanta, GA 30346. The California Air Resources Board contributed support for travel expenses incurred during the Fall study measurements.

REFERENCES

1. Marple V.A. and Rubow K.L. (1984) Final Report on DOE Contract No. DE–FG22–83PC61255, Dept. Mech. Eng., Univ. of MN, 111 Church St. SE, Minneapolis, MN 55455.

2. Mueller P.K., Fung K.K., Heisler S.L. Grosjean D. and Hidy G.M. (1982) in Particulate Carbon: Atmospheric Life Cycle, G.T. Wolff, T.L. Klimisch, Eds, Plenum Press, NY.

3. McMurry P.H. and Zhang X.Q. (1989) Size distributions of ambient organic and elemental carbon. Aerosol Sci. Technol., 10:430–437.

4. John W. and Reischl G. (1980) J. Air Pollut. Control Assoc. 30:872.

5. McMurry, P.H. and X.Q. Zhang (1988) The Carbonaceous Species Methods Comparison Study: University of Minnesota Results, Report to the Coordinating Research Council Inc, 219 Perimeter Center Parkway, Atlanta, GA 30346.

6. A.C. Szkarlat and S.M. Japar (1981) Light absorption by airborne aerosols: comparison of integrating plate and spectrophone techniques, Applied Optics 20:1151–1154.

7. Hansen, A.D.A., H. Rosen, and T. Novakov (1984) The Aethalometer–an instrument for the real–time measurement of optical absorption by aerosol particles, Sci. Total Environ. 36:191–194.

APPENDIX I

SUMMARY OF MOUDI SAMPLES ACQUIRED DURING SCAQS

CLAREMONT SAMPLES

Date	Julian Date	Sample ID	Start Time	Stop Time	Elapsed Time(min)	Volume (m^3)
19–JUN–87	170	CL–MN–MI–170	06:18	09:32	188	5.55
19–JUN–87	170	CL–MN–MI–170	10:01	13:33	212	6.25
19–JUN–87	170	CL–MN–MI–170	14:13	17:32	199	5.87
19–JUN–87	170	CL–MN–MI–170	18:14	01:00	406	12.0
24–JUN–87	175	CL–MN–MI–175	06:00	09:40	220	6.60
24–JUN–87	175	CL–MN–MI–175	10:01	13:34	213	6.39
24–JUN–87	175	CL–MN–MI–175	14:00	17:33	213	6.39
24–JUN–87	175	CL–MN–MI–175	18:00	05:33	693	20.7
25–JUN–87	176	CL–MN–MI–176	06:00	09:30	210	6.30
25–JUN–87	176	CL–MN–MI–176	10:05	13:36	211	6.33
25–JUN–87	176	CL–MN–MI–176	14:00	17:33	213	6.39
25–JUN–87	176	CL–MN–MI–176	18:00	01:00	420	12.6
13–JUL–87	194	CL–MN–MI–194	06:00	09:39	219	6.62
13–JUL–87	194	CL–MN–MI–194	10:07	13:33	206	6.63
13–JUL–87	194	CL–MN–MI–194	14:05	17:44	219	6.62
13–JUL–87	194	CL–MN–MI–194	18:20	05:29	669	20.2
14–JUL–87	195	CL–MN–MI–195	06:00	09:39	219	6.57
14–JUL–87	195	CL–MN–MI–195	10:00	13:30	210	6.30
14–JUL–87	195	CL–MN–MI–195	14:00	17:30	210	6.30
14–JUL–87	195	CL–MN–MI–195	18:00	05:30	690	20.7
15–JUL–87	196	CL–MN–MI–196	06:00	09:37	217	6.36
15–JUL–87	196	CL–MN–MI–196	10:22	13:38	196	6.02
15–JUL–87	196	CL–MN–MI–196	14:00	17:30	210	6.30
15–JUL–87	196	CL–MN–MI–196	18:00	01:00	420	12.7
27–AUG–87	239	CL–MN–MI–239	06:07	09:49	222	6.68
27–AUG–87	239	CL–MN–MI–239	10:01	13:46	225	6.77
27–AUG–87	239	CL–MN–MI–239	13:54	17:48	234	7.04
27–AUG–87	239	CL–MN–MI–239	17:56	05:50	714	21.5
28–AUG–87	240	CL–MN–MI–240	06:02	09:44	222	6.68
28–AUG–87	240	CL–MN–MI–240	09:52	13:39	227	6.83
28–AUG–87	240	CL–MN–MI–240	13:47	17:51	244	7.34
28–AUG–87	240	CL–MN–MI–240	18:00	05:50	710	21.5
29–AUG–87	241	CL–MN–MI–241	05:58	09:56	238	7.16
29–AUG–87	241	CL–MN–MI–241	10:04	13:43	219	6.59
29–AUG–87	241	CL–MN–MI–241	13:50	17:50	240	7.22
29–AUG–87	241	CL–MN–MI–241	17:56	00:53	417	12.6
02–SEP–87	245	CL–MN–MI–245	06:00	09:50	230	6.92
02–SEP–87	245	CL–MN–MI–245	09:56	13:48	232	6.98
02–SEP–87	245	CL–MN–MI–245	13:53	17:59	246	7.38
02–SEP–87	245	CL–MN–MI–245	18:09	05:54	705	21.2
03–SEP–87	246	CL–MN–MI–246	06:01	09:54	233	7.01
03–SEP–87	246	CL–MN–MI–246	10:00	13:49	229	6.89
03–SEP–87	246	CL–MN–MI–246	13:57	17:46	229	6.89
03–SEP–87	246	CL–MN–MI–246	17:54	00:30	396	11.9

RUBIDOUX SAMPLES

Date	Julian Date	Sample ID	Start Time	Stop Time	Elapsed Time(min)	Volume (m^3)
19–JUN–87	170	RB–MN–MI–170	06:05	09:32	207	6.25
19–JUN–87	170	RB–MN–MI–170	10:05	13:45	200	6.04
19–JUN–87	170	RB–MN–MI–170	14:00	17:30	210	6.43
19–JUN–87	170	RB–MN–MI–170	18:25	01:00	395	11.1
24–JUN–87	175	RB–MN–MI–175	06:16	09:30	194	5.72
24–JUN–87	175	RB–MN–MI–175	10:00	13:37	217	6.73
24–JUN–87	175	RB–MN–MI–175	14:00	17:37	217	6.73
24–JUN–87	175	RB–MN–MI–175	18:00	05:42	702	21.8
25–JUN–87	176	RB–MN–MI–176	06:00	09:30	210	6.43
25–JUN–87	176	RB–MN–MI–176	10:00	13:30	210	6.51
25–JUN–87	176	RB–MN–MI–176	14:00	17:30	210	6.52
25–JUN–87	176	RB–MN–MI–176	18:00	01:00	420	13.0
13–JUL–87	194	RB–MN–MI–194	05:58	09:40	222	6.88
13–JUL–87	194	RB–MN–MI–194	09:58	13:28	210	6.51
13–JUL–87	194	RB–MN–MI–194	13:50	17:25	215	6.67
13–JUL–87	194	RB–MN–MI–194	17:50	05:32	702	21.0
14–JUL–87	195	RB–MN–MI–195	06:00	09:28	208	6.45
14–JUL–87	195	RB–MN–MI–195	10:00	13:34	214	6.63
14–JUL–87	195	RB–MN–MI–195	14:00	17:35	215	6.67
14–JUL–87	195	RB–MN–MI–195	18:00	05:40	700	21.7
15–JUL–87	196	RB–MN–MI–196	05:58	09:32	214	6.63
15–JUL–87	196	RB–MN–MI–196	09:58	13:40	222	6.88
15–JUL–87	196	RB–MN–MI–196	14:00	17:30	210	6.51
15–JUL–87	196	RB–MN–MI–196	18:00	01:00	420	13.0
27–AUG–87	239	RB–MN–MI–239	05:55	09:30	215	6.69
27–AUG–87	239	RB–MN–MI–239	10:00	13:33	213	6.65
27–AUG–87	239	RB–MN–MI–239	14:00	17:30	210	6.55
27–AUG–87	239	RB–MN–MI–239	18:00	05:40	700	21.5
28–AUG–87	240	RB–MN–MI–240	06:00	09:40	220	6.75
28–AUG–87	240	RB–MN–MI–240	10:00	13:40	220	6.75
28–AUG–87	240	RB–MN–MI–240	14:00	17:35	215	6.60
28–AUG–87	240	RB–MN–MI–240	18:00	05:40	700	21.5
29–AUG–87	241	RB–MN–MI–241	06:00	09:35	215	6.60
29–AUG–87	241	RB–MN–MI–241	10:00	13:40	220	6.75
29–AUG–87	241	RB–MN–MI–241	14:00	17:40	220	6.84
29–AUG–87	241	RB–MN–MI–241	18:00	01:00	420	12.9
02–SEP–87	245	RB–MN–MI–245	06:00	09:35	215	6.69
02–SEP–87	245	RB–MN–MI–245	10:00	13:40	220	6.75
02–SEP–87	245	RB–MN–MI–245	14:00	17:40	220	6.75
02–SEP–87	245	RB–MN–MI–245	18:00	05:40	700	21.0
03–SEP–87	246	RB–MN–MI–246	06:00	09:40	220	6.84
03–SEP–87	246	RB–MN–MI–246	10:00	13:40	220	6.84
03–SEP–87	246	RB–MN–MI–246	14:00	17:40	220	6.60
03–SEP–87	246	RB–MN–MI–246	18:00	01:05	425	13.0

Los Angeles Samples

Date	Julian Date	Sample ID	Start Time	Stop Time	Elapsed Time(min)	Volume (m^3)
11–NOV–87	315	LA–MN–MI–307	06:27	09:30	183	5.49
11–NOV–87	315	LA–MN–MI–307	10:00	13:30	210	6.30
11–NOV–87	315	LA–MN–MI–307	14:00	17:30	210	6.30
11–NOV–87	315	LA–MN–MI–307	18:00	05:30	690	20.7
12–NOV–87	316	LA–MN–MI–308	06:00	09:30	210	6.30
12–NOV–87	316	LA–MN–MI–308	10:00	13:30	210	6.30
12–NOV–87	316	LA–MN–MI–308	14:00	17:30	210	6.30
12–NOV–87	316	LA–MN–MI–308	18:00	05:30	690	20.7
13–NOV–87	317	LA–MN–MI–309	06:00	09:30	210	6.30
13–NOV–87	317	LA–MN–MI–309	10:00	13:30	210	6.30
13–NOV–87	317	LA–MN–MI–309	14:00	17:30	210	6.30
13–NOV–87	317	LA–MN–MI–309	18:00	00:00	360	10.8
03–DEC–87	337	LA–MN–MI–329	06:00	09:30	210	6.30
03–DEC–87	337	LA–MN–MI–329	10:00	13:30	210	6.30
03–DEC–87	337	LA–MN–MI–329	14:00	17:30	210	6.30
03–DEC–87	337	LA–MN–MI–329	18:00	00:00	360	10.8
10–DEC–87	344	LA–MN–MI–336	06:00	09:30	210	6.30
10–DEC–87	344	LA–MN–MI–336	10:00	13:30	210	6.30
10–DEC–87	344	LA–MN–MI–336	14:00	17:30	210	6.30
10–DEC–87	344	LA–MN–MI–336	18:00	05:30	690	20.7
11–DEC–87	345	LA–MN–MI–337	06:00	09:30	210	6.30
11–DEC–87	345	LA–MN–MI–337	10:00	13:30	210	6.30
11–DEC–87	345	LA–MN–MI–337	14:00	17:30	210	6.30
11–DEC–87	345	LA–MN–MI–337	18:00	00:00	240	7.20

LONG BEACH SAMPLES

Date	Julian Date	Sample ID	Start Time	Stop Time	Elapsed Time(min)	Volume (m^3)
11–NOV–87	315	LB–MN–MI–307	06:00	09:30	210	6.30
11–NOV–87	315	LB–MN–MI–307	10:00	13:30	210	6.30
11–NOV–87	315	LB–MN–MI–307	14:00	17:30	210	6.30
11–NOV–87	315	LB–MN–MI–307	18:00	05:30	690	20.7
12–NOV–87	316	LB–MN–MI–308	06:00	09:30	210	6.30
12–NOV–87	316	LB–MN–MI–308	10:00	13:30	210	6.30
12–NOV–87	316	LB–MN–MI–308	14:00	17:30	210	6.30
12–NOV–87	316	LB–MN–MI–308	18:00	05:30	690	20.7
13–NOV–87	317	LB–MN–MI–308	06:00	09:30	210	6.30
13–NOV–87	317	LB–MN–MI–309	10:00	13:30	210	6.30
13–NOV–87	317	LB–MN–MI–309	14:00	17:30	210	6.30
13–NOV–87	317	LB–MN–MI–309	18:00	00:00	360	10.8
03–DEC–87	337	LB–MN–MI–329	06:00	09:30	210	6.30
03–DEC–87	337	LB–MN–MI–329	10:00	13:30	210	6.30
03–DEC–87	337	LB–MN–MI–329	14:00	17:30	210	6.30
03–DEC–87	337	LB–MN–MI–329	18:00	00:00	360	10.8
10–DEC–87	344	LB–MN–MI–329	06:00	09:30	210	6.30
10–DEC–87	344	LB–MN–MI–336	10:00	13:30	210	6.30
10–DEC–87	344	LB–MN–MI–336	14:00	17:30	210	6.30
10–DEC–87	344	LB–MN–MI–336	18:00	05:00	690	20.7
11–DEC–87	345	LB–MN–MI–336	06:00	09:30	210	6.30
11–DEC–87	345	LB–MN–MI–337	10:00	13:30	210	6.30
11–DEC–87	345	LB–MN–MI–337	14:00	17:30	210	6.30
11–DEC–87	345	LB–MN–MI–337	18:00	00:00	360	10.8

APPENDIX II

SIZE–DEPENDENT COLLECTION EFFICIENCIES FOR MOUDI STAGES DURING SCAQS

Two MOUDIs were used during SCAQS. Impactor I was used at Claremont and Long Beach, and Impactor II was used at Rubidoux and Los Angeles. The calibration history of these impactors during SCAQS is summarized in this appendix.

Impactor I (Rubidoux and Los Angeles)

The pressure drop (from atmospheric) measured after stage 8 decreased slightly during a rainstorm on the morning of Sept. 2. A subsequent examination of the stage 8 orifice plate indicated that a cluster of 5–10 orifices had enlarged slightly (there are a total of 2000 orifices on stage 8). The reason for this change in hole size is unknown, but we have speculated that it was associated with the high moisture levels on that day. The orifices were formed by a chemical etching process, and it it may be that that portion of the plate was not adequately rinsed during the manufacturing process.

The calibration of stage 8 was checked between summer and fall SCAQS measurements to determine whether or not the change in pressure affected size cuts for that stage. It was found that size cuts were somewhat affected. The enlarged holes were plugged, and the resulting collection efficiencies returned to the original values.

In reducing SCAQS data it is assumed that collection efficiencies up to the morning of September 2 are the same as those determined before leaving for the field. The eight size distributions measured on September 2 and 3 (at the end of summer SCAQS) have different collection efficiencies on stage 8. Collection efficiencies return to the original values for fall measurements. Values for collection efficiencies are given in Table AI.

Impactor II (Claremont and Long Beach)

A minor adjustment to the jet–to–plate spacing on stages 7 and 8 was made between summer and fall measurements. This somewhat modified the size–dependent collection efficiencies for those stages. The collection efficiencies that were used in inverting fall and summer data are, therefore, somewhat different. Values for size dependent collection efficiencies are given in Table AII.

Table AI. MOUDI I Collection Efficiencies[1]

Stage 1 (D_{50} = 3.2 μm)

Dp, μm	η
2.8	0.0
2.98	0.34
3.12	0.54
3.26	0.83
3.4	0.94

Stage 2 (D_{50} = 1.8 μm)

Dp, μm	η
1.38	0.021
1.64	0.279
1.77	0.587
1.87	0.862
2.05	0.967

Stage 3 (D_{50} = 1.0 μm)

Dp, μm	η
0.79	0.0209
0.94	0.279
1.01	0.587
1.07	0.862
1.17	0.967

Stage 4 (D_{50} = 0.56 μm)

Dp, μm	η
0.66	0.98
0.61	0.88
0.60	0.73
0.58	0.58
0.56	0.49
0.53	0.25
0.50	0.16
0.45	0.08

Stage 5 (D50 = 0.28 μm)

Dp, μm	η
0.35	0.90
0.33	0.86
0.30	0.76
0.28	0.53
0.27	0.45
0.26	0.34
0.25	0.27
0.22	0.08

Stage 6 (D50 = 0.17 μm)

Dp, μm	η
0.25	0.91
0.20	0.82
0.18	0.62
0.17	0.50
0.15	0.22
0.13	0.15
0.10	0.10

[1]Stage 3 (nominal size cut = 1.0 μm) was not calibrated due to the difficulty of producing monodisperse particles in this size range. Instead, the D_{50} for this stage was estimated from theory, and the shape of the collection efficiency curve was assumed to be identical to that for stage 2. This approach should introduce negligible uncertainty into the data since impactor theory in this flow regime is well established.

Table AI, continued

Stage 7 (D_{50} = 0.072 μm)

Dp, μm	η
0.20	1.00
0.14	0.97
0.090	0.78
0.080	0.67
0.070	0.48
0.060	0.30

Stage 8 (D_{50} = 0.036 μm)

Dp, μm	η
0.12	0.98
0.10	0.95
0.090	0.93
0.080	0.91
0.070	0.84
0.060	0.80
0.050	0.68
0.040	0.58
0.030	0.38

Anomalous Efficiency Data for MOUDI I (to be used for the eight samples collected on Julian Dates 245 and 246).

Stage 7 (D_{50} = 0.08 μm)

Dp, μm	η
0.15	0.96
0.12	0.87
0.10	0.77
0.090	0.66
0.080	0.49
0.070	0.36
0.060	0.16

Stage 8 (D_{50} = 0.068 μm)

Dp, μm	η
0.20	0.93
0.15	0.89
0.12	0.85
0.10	0.75
0.080	0.61
0.070	0.51
0.060	0.38

Table AII. MOUDI II Collection Efficiencies[2]

Stages 1,2,3 are identical to MOUDI I and remained constant during SCAQS

Stage 4 (D_{50} = 0.56 μm)

Dp, μm	η
0.66	0.98
0.61	0.88
0.59	0.75
0.58	0.62
0.56	0.53
0.53	0.34
0.50	0.20
0.45	0.09

Stage 5 (D_{50} = 0.28 μm)

Dp, μm	η
0.40	0.95
0.35	0.90
0.30	0.71
0.29	0.64
0.28	0.51
0.27	0.43
0.26	0.33
0.30	0.26
0.22	0.08

Stage 6 (D_{50} = 0.19 μm)

Dp, μm	η
0.28	0.94
0.25	0.92
0.22	0.87
0.20	0.66
0.51	0.19
0.18	0.39
0.16	0.22
0.13	0.16

Stage 7 (D_{50} = 0.062 μm)

Dp, μm	η
0.15	0.96
0.13	0.95
0.12	0.94
0.10	0.90
0.080	0.80
0.070	0.62
0.060	0.50
0.050	0.29

Stage 8 (D_{50} = 0.034 μm)

Dp, μm	η
0.12	1.00
0.10	0.97
0.080	0.94
0.060	0.86
0.040	0.45

[2]Stage 3 (nominal size cut = 1.0 μm) was not calibrated due to the difficulty of producing monodisperse particles in this size range. Instead, the D_{50} for this stage was estimated from theory, and the shape of the collection efficiency curve was assumed to be identical to that for stage 2. This approach should introduce negligible uncertainty into the data since impactor theory in this flow regime is well established.

Table IIA, continued.

MOUDI II efficiency curves for stages 7 and 8 to be used on samples collected on Julian Dates 170 thru 246 (summer SCAQS measurements)

Stage 7 (D_{50} = 0.086 μm)

Dp, μm	η
0.15	0.78
0.12	0.74
0.10	0.64
0.090	0.55
0.080	0.39
0.070	0.23
0.060	0.18

Stage 8 (D_{50} = 0.046 μm)

Dp, μm	η
0.10	0.84
0.080	0.79
0.070	0.75
0.060	0.68
0.050	0.50
0.040	0.43

APPENDIX III

LOADINGS ON MOUDI STAGES FOR SCAQS MEASUREMENTS

A separate page is included for each intensive sampling date during SCAQS. Data from the upwind site (Claremont or Long Beach) is shown at the top of the page, and data from the downwind site (Rubidoux or Los Angeles) is on the bottom. Two columns are identified for each data set. The first column is residual organic carbon (ROC) and the second column is elemental carbon (EC). Indicated sampling intervals are nominal, although the tabulated values for the volume of air sampled are the actual volumes sampled.

For reasons that we have not been able to ascertain, some of the afterfilters were lost. A value of 0.0 for ROC afterfilters loadings indicates that no afterfilter was found to be analyzed. Our standard handling sampling procedure involved packing the afterfilters with the stage substrates. Since all stage substrates were delivered to ERT, we also believe all afterfilters were delivered.

The omission of the afterfilters is not a serious problem. The amount of particulate matter collected by the afterfilters is negligible since only a small fraction of particulate matter is in sizes smaller than the cut size of the bottom stage. In previous work we often found high ROC loadings on afterfilters. Arguments were presented by McMurry and Zhang (1988) which suggest that most of this material is associated with vapor adsorption on the afterfilter.

Sample ID	CL-ER-MD-170-0618-0932		CL-ER-MD-170-1001-1333		CL-ER-MD-170-1413-1732		CL-ER-MD-170-1814-0100	
Julian Start Date	170		170		170		170	
Calendar Start Date	Jun 19		Jun 19		Jun 19		Jun 19	
Start time	0618-0932		1001-1333		1413-1732		1814-0100	
Volume (m3)	5.55		6.25		5.87		12.0	
Stage 1 (ug/stage)	1.09	0.00	0.00	0.00	3.00	0.00	0.46	1.20
2	0.49	0.00	0.39	0.00	1.59	0.00	1.99	1.13
3	3.96	0.00	4.97	0.00	2.03	0.00	4.30	0.00
4	7.63	1.44	4.63	1.49	5.86	0.63	5.12	1.12
5	22.61	5.08	15.84	4.99	12.76	5.19	16.01	5.51
6	15.09	5.93	10.73	4.42	9.81	2.97	17.22	5.47
7	12.18	4.69	8.08	2.56	8.68	1.29	13.37	5.04
8	3.57	1.25	3.51	0.00	4.77	0.00	5.36	1.48
AF	0.00	0.00	0.00	0.00	0.00	0.00	0.00	0.00

Sample ID	RB-ER-MD-170-0605-0932		RB-ER-MD-170-1005-1345		RB-ER-MD-170-1400-1730		RB-ER-MD-170-1825-0100	
Julian Start Date	170		170		170		170	
Calendar Start Date	Jun 19		Jun 19		Jun 19		Jun 19	
Start time	0605-0932		1005-1345		1400-1730		1825-0100	
Volume (m3)	6.25		6.04		6.43		11.1	
Stage 1 (ug/stage)	0.00	0.00	0.00	0.00	0.00	0.00	0.00	0.00
2	1.75	0.00	6.25	0.00	0.00	0.00	1.19	0.00
3	3.78	0.00	6.47	0.00	3.36	0.00	3.46	0.00
4	7.25	1.50	3.17	1.35	0.98	0.00	0.36	0.00
5	11.42	4.51	7.94	3.74	6.53	2.44	10.32	1.58
6	11.30	4.50	6.02	3.11	5.83	1.31	7.55	1.25
7	11.34	4.28	1.31	0.00	0.47	0.00	0.86	1.85
8	0.00	0.00	0.00	0.00	0.00	0.00	0.00	0.00
AF	0.00	0.00	0.00	0.00	0.00	0.00	0.00	0.00

Sample ID	CL-ER-MD-175-0600-0940		CL-ER-MD-175-1001-1334		CL-ER-MD-175-1413-1732		CL-ER-MD-175-1814-0533	
Julian Start Date	175		175		175		175	
Calendar Start Date	Jun 24		Jun 24		Jun 24		Jun 24	
Start time	0600-0940		1001-1334		1413-1732		1814-0533	
Volume (m3)	6.60		6.39		6.39		20.7	
Stage 1 (ug/stage)	0.00	0.00	1.53	0.00	1.54	0.00	8.75	0.00
2	0.16	0.00	1.54	0.00	0.23	0.00	3.28	0.00
3	4.39	2.76	4.37	1.43	4.60	1.34	5.88	0.00
4	9.53	4.05	12.53	4.64	24.34	4.91	17.58	6.29
5	12.74	5.85	22.81	9.77	27.65	8.17	25.53	6.61
6	13.40	5.52	15.51	6.32	22.19	4.61	16.16	10.30
7	7.67	3.39	11.51	3.66	12.90	2.28	16.82	10.11
8	7.69	1.37	7.61	1.33	3.20	1.02	8.44	2.00
AF	0.00	0.00	0.00	0.00	0.00	0.00	0.00	0.00

Sample ID	RB-ER-MD-175-0616-0930		RB-ER-MD-175-1000-1337		RB-ER-MD-175-1400-1737		RB-ER-MD-175-1800-0542	
Julian Start Date	175		175		175		175	
Calendar Start Date	Jun 24		Jun 24		Jun 24		Jun 24	
Start time	0616-0930		1000-1337		1400-1737		1800-0542	
Volume (m3)	5.72		6.73		6.73		21.8	
Stage 1 (ug/stage)	0.00	0.00	0.00	0.00	0.00	0.00	0.31	0.00
2	2.18	0.00	3.04	0.00	0.00	0.00	4.28	0.00
3	11.03	1.60	24.75	6.14	13.78	1.55	6.13	2.77
4	7.88	1.88	11.61	8.08	0.47	1.02	11.37	4.09
5	5.11	2.82	22.05	14.42	13.51	4.92	15.12	11.70
6	7.82	3.00	10.87	8.65	3.83	2.36	12.67	11.55
7	3.06	3.55	5.85	1.59	3.09	1.22	10.58	3.87
8	0.00	0.00	0.00	0.00	0.00	0.00	0.00	0.00
AF	0.00	0.00	0.00	0.00	0.00	0.00	0.00	0.00

Sample ID	CL-ER-MD-176-0600-0930		CL-ER-MD-176-1005-1336		CL-ER-MD-176-1400-1733		CL-ER-MD-176-1800-0100	
Julian Start Date	176		176		176		176	
Calendar Start Date	Jun 25		Jun 25		Jun 25		Jun 25	
Start time	0600-0930		1005-1336		1400-1733		1800-0100	
Volume (m3)	6.30		6.33		6.39		12.60	
Stage 1 (ug/stage)	4.31	0.00	2.65	0.00	2.16	0.00	2.84	0.00
2	0.21	0.00	1.09	0.00	0.13	0.00	0.79	0.00
3	5.26	1.20	8.86	1.53	3.95	0.00	1.99	0.00
4	12.57	3.78	22.71	3.99	7.06	2.43	15.03	2.36
5	28.26	12.96	38.65	11.96	17.41	8.31	24.65	6.30
6	17.31	12.39	16.41	8.34	16.15	7.34	15.40	5.86
7	12.89	6.93	15.21	2.66	9.72	2.73	15.63	4.09
8	7.57	2.31	2.14	0.00	4.30	0.00	8.42	1.23
AF	0.00	0.00	0.00	0.00	0.00	0.00	0.00	0.00

Sample ID	RB-ER-MD-176-0600-0930		RB-ER-MD-176-1000-1330		RB-ER-MD-176-1400-1730		RB-ER-MD-176-1800-0100	
Julian Start Date	176		176		176		176	
Calendar Start Date	Jun 25		Jun 25		Jun 25		Jun 25	
Start time	0600-0930		1000-1330		1400-1730		1800-0100	
Volume (m3)	6.43		6.51		6.52		13.0	
Stage 1 (ug/stage)	0.00	0.00	1.88	0.00	0.00	0.00	1.05	0.00
2	0.77	0.00	0.00	0.00	0.00	0.00	0.00	0.00
3	4.07	2.14	7.73	1.13	6.12	1.51	13.19	1.21
4	3.77	1.37	13.91	6.07	3.18	1.90	6.37	4.46
5	1.11	3.49	6.69	4.52	10.77	3.87	15.96	6.03
6	8.36	5.88	5.48	4.14	8.08	2.61	15.29	6.12
7	0.78	3.11	0.00	0.00	0.09	0.00	4.55	2.39
8	0.00	0.00	0.00	0.00	4.16	0.00	0.85	0.00
AF	0.00	0.00	0.00	0.00	0.00	0.00	0.00	0.00

Sample ID	CL-ER-MD-194-0600-0939		CL-ER-MD-194-1007-1333		CL-ER-MD-194-1405-1744		CL-ER-MD-194-1820-0529	
Julian Start Date	194		194		194		194	
Calendar Start Date	Jul 13		Jul 13		Jul 13		Jul 13	
Start time	0600-0939		1007-1333		1405-1744		1820-0529	
Volume (m3)	6.62		6.63		6.62		20.2	
Stage 1 (ug/stage)	0.81	0.00	1.96	0.00	1.89	0.00	3.08	0.00
2	0.00	0.00	0.04	0.00	0.00	0.00	0.20	0.00
3	1.18	0.30	0.22	0.00	0.00	0.00	1.24	0.00
4	15.69	2.37	11.19	1.25	6.29	0.00	15.25	1.80
5	21.95	7.27	24.24	5.86	21.66	6.43	23.68	2.89
6	21.56	7.24	19.63	6.24	20.23	4.22	21.69	4.15
7	14.20	6.20	10.02	4.17	13.93	3.25	19.42	5.59
8	5.79	2.34	2.05	0.00	3.27	0.54	10.26	1.97
AF	0.00	0.00	0.00	0.00	0.00	0.00	0.00	0.00

Sample ID	RB-ER-MD-194-0558-0940		RB-ER-MD-194-0958-1328		RB-ER-MD-194-1350-1725		RB-ER-MD-194-1750-0532	
Julian Start Date	194		194		194		194	
Calendar Start Date	Jul 13		Jul 13		Jul 13		Jul 13	
Start time	0558-0940		0958-1328		1350-1725		1750-0532	
Volume (m3)	6.88		6.51		6.67		21.0	
Stage 1 (ug/stage)	4.16	0.00	0.00	0.00	1.94	0.00	0.00	0.00
2	0.00	0.00	0.00	0.00	0.00	0.00	0.00	0.00
3	8.55	5.17	2.38	0.00	2.99	0.00	0.00	0.00
4	9.17	5.45	3.23	0.00	2.83	0.00	4.25	1.78
5	11.80	7.20	11.73	2.65	15.13	2.08	23.45	7.77
6	14.97	8.03	4.21	1.65	5.57	0.00	21.75	9.02
7	5.07	3.73	0.55	0.00	0.40	0.00	12.25	8.63
8	0.00	0.00	0.00	0.00	1.68	0.00	0.00	0.00
AF	0.00	0.00	0.00	0.00	0.00	0.00	0.00	0.00

Sample ID	CL-ER-MD-195-0600-0939		CL-ER-MD-195-1000-1330		CL-ER-MD-195-1400-17330		CL-ER-MD-195-1800-0530	
Julian Start Date	195		195		195		195	
Calendar Start Date	Jul 14		Jul 14		Jul 14		Jul 14	
Start time	0600-0939		1000-1330		1400-17330		1800-0530	
Volume (m3)	6.57		6.30		6.30		20.70	
Stage 1 (ug/stage)	0.97	0.00	0.00	0.00	1.60	0.00	0.70	0.00
2	0.00	0.00	0.00	0.00	0.00	0.00	0.00	0.00
3	0.01	0.00	0.24	0.00	3.20	0.00	6.15	1.21
4	6.07	1.27	10.13	3.34	9.78	1.90	21.66	4.98
5	13.43	4.38	17.90	5.61	19.00	7.27	25.81	7.13
6	10.71	4.76	11.34	4.23	15.57	7.02	10.89	4.01
7	10.28	3.55	7.43	3.14	7.98	2.33	10.99	2.45
8	2.44	0.00	2.51	0.00	1.61	0.00	5.14	0.00
AF	0.00	0.00	0.00	0.00	0.00	0.00	0.00	0.00

Sample ID	RB-ER-MD-195-0600-0928		RB-ER-MD-195-1000-1334		RB-ER-MD-195-1400-1735		RB-ER-MD-195-1800-0540	
Julian Start Date	195		195		195		195	
Calendar Start Date	Jul 14		Jul 14		Jul 14		Jul 14	
Start time	0600-0928		1000-1334		1400-1735		1800-0540	
Volume (m3)	6.45		6.63		6.6		21.00	
Stage 1 (ug/stage)	4.17	0.00	0.00	0.00	0.00	0.00	0.00	0.00
2	0.00	0.00	0.00	0.00	0.26	0.00	0.00	0.00
3	0.00	0.00	2.35	0.00	3.08	1.51	6.17	1.20
4	5.01	0.00	6.15	2.20	6.00	5.23	15.22	8.77
5	8.72	6.10	9.32	9.70	13.87	10.80	15.22	8.31
6	4.95	8.11	6.71	3.45	4.50	3.57	8.45	6.21
7	5.24	7.38	2.32	2.74	1.70	0.00	5.60	5.03
8	0.00	0.00	0.00	0.00	1.49	0.00	3.57	0.00
AF	0.00	0.00	0.00	0.00	0.00	0.00	0.00	0.00

Sample ID	CL-ER-MD-196-0600-0937		CL-ER-MD-196-1022-1338		CL-ER-MD-196-1400-1730		CL-ER-MD-196-1800-0100	
Julian Start Date	196		196		196		196	
Calendar Start Date	Jul 15		Jul 15		Jul 15		Jul 15	
Start time	0600-0937		1022-1338		1400-1730		1800-0100	
Volume (m3)	6.31		6.02		6.30		12.7	
Stage 1 (ug/stage)	1.49	0.00	0.93	0.00	1.20	0.00	1.03	0.00
2	1.56	0.00	0.55	0.00	0.32	0.00	0.00	0.00
3	2.92	0.00	2.33	0.00	1.44	0.00	2.06	0.00
4	8.32	0.60	22.82	3.38	10.36	1.59	16.30	3.58
5	13.09	5.36	21.58	5.70	19.06	4.77	25.99	6.55
6	10.82	3.72	8.33	3.92	8.12	2.74	17.83	5.62
7	6.29	1.34	3.32	1.20	5.71	1.39	8.47	2.46
8	0.00	0.00	2.03	0.00	1.09	0.00	5.69	0.00
AF	0.00	0.00	0.00	0.00	0.00	0.00	0.00	0.00

Sample ID	RB-ER-MD-196-0558-0932		RB-ER-MD-196-0958-1340		RB-ER-MD-196-1400-1730		RB-ER-MD-196-1800-0100	
Julian Start Date	196		196		196		196	
Calendar Start Date	Jul 15		Jul 15		Jul 15		Jul 15	
Start time	0558-0932		0958-1340		1400-1730		1800-0100	
Volume (m3)	6.63		6.88		6.51		13.0	
Stage 1 (ug/stage)	0.00	0.00	3.20	0.00	0.00	0.00	0.00	0.00
2	1.33	0.00	0.00	0.00	0.00	0.00	0.00	0.00
3	3.09	2.53	10.25	1.31	0.01	0.00	2.00	0.00
4	6.20	2.66	22.34	9.54	0.16	0.57	13.33	7.12
5	4.91	3.98	10.19	6.82	15.22	7.92	10.90	10.21
6	1.85	2.38	4.47	3.57	4.27	1.38	10.25	6.34
7	1.42	0.00	2.53	0.00	6.13	1.10	0.40	0.00
8	0.00	0.00	0.62	0.00	0.00	0.00	0.00	0.00
AF	0.00	0.00	0.00	0.00	0.00	0.00	0.00	0.00

Sample ID	CL-ER-MD-239-0607-0949		CL-ER-MD-239-1001-1346		CL-ER-MD-239-1354-1748		CL-ER-MD-239-1756-0550	
Julian Start Date	239		239		239		239	
Calendar Start Date	Aug 27		Aug 27		Aug 27		Aug 27	
Start time	0607-0949		1001-1346		1354-1748		1756-0550	
Volume (m3)	6.68		6.67		7.04		21.5	
Stage 1 (ug/stage)	0.00	0.00	0.00	0.00	0.00	0.00	0.00	0.00
2	0.00	0.00	0.00	0.00	0.00	0.00	0.00	0.00
3	2.36	1.28	1.21	0.00	0.00	0.00	7.12	0.00
4	2.74	0.00	0.00	0.00	7.60	1.47	10.46	2.89
5	10.39	6.51	3.48	2.42	25.48	10.52	33.31	6.02
6	7.50	6.66	10.69	9.57	16.65	6.17	12.74	10.93
7	4.85	7.20	10.40	2.72	10.39	0.00	14.74	0.00
8	0.31	0.00	0.00	0.00	0.00	0.00	4.23	3.58
AF	20.10	0.70	36.20	1.10	46.90	2.10	37.70	2.00

Sample ID	RB-ER-MD-239-0555-0930		RB-ER-MD-239-1000-1330		RB-ER-MD-239-1400-1730		RB-ER-MD-239-1800-0540	
Julian Start Date	239		239		239		239	
Calendar Start Date	Aug 27		Aug 27		Aug 27		Aug 27	
Start time	0555-0930		1000-1330		1400-1730		1800-0540	
Volume (m3)	6.69		6.65		6.55		21.5	
Stage 1 (ug/stage)	0.00	0.00	0.18	0.00	1.99	0.00	0.00	0.00
2	0.42	0.00	0.00	0.00	0.00	0.00	0.00	0.00
3	0.00	0.00	3.68	0.00	0.30	0.00	10.01	1.79
4	12.59	0.00	12.42	1.58	7.66	4.00	14.62	6.69
5	11.94	8.03	11.06	5.75	13.28	6.20	35.36	11.13
6	8.04	8.74	3.09	0.00	15.40	8.98	23.94	19.92
7	10.29	10.40	3.17	1.27	3.11	0.00	10.98	12.14
8	0.07	0.00	0.51	0.00	1.32	0.00	0.80	0.00
AF	23.45	1.00	33.60	1.50	43.55	2.90	34.40	1.40

Sample ID	CL-ER-MD-240-0602-0944		CL-ER-MD-240-952-1339		CL-ER-MD-240-1347-1751		CL-ER-MD-240-1800-0550	
Julian Start Date	240		240		240		240	
Calendar Start Date	Aug 28		Aug 28		Aug 28		Aug 28	
Start time	0602-0944		952-1339		1347-1751		1800-0550	
Volume (m3)	6.68		6.83		7.34		21.5	
Stage 1 (ug/stage)	0.00	0.00	0.00	0.00	0.78	0.00	1.01	0.00
2	0.00	0.00	0.83	0.00	0.00	0.00	0.17	0.00
3	3.40	3.23	0.00	0.00	3.98	0.00	3.75	0.00
4	1.48	0.00	10.31	3.29	0.00	0.00	13.87	3.75
5	7.59	6.01	14.01	13.67	28.16	6.49	42.79	25.06
6	6.18	7.94	7.18	1.08	19.92	6.75	23.33	20.01
7	4.70	1.67	4.31	4.38	7.68	0.96	11.71	11.98
8	0.00	0.00	0.25	0.00	0.00	0.00	4.51	0.00
AF	20.80	1.10	32.30	1.20	52.60	1.90	28.60	1.80

Sample ID	RB-ER-MD-240-0600-0940		RB-ER-MD-240-1000-1340		RB-ER-MD-240-1400-1735		RB-ER-MD-240-1800-0540	
Julian Start Date	240		240		240		240	
Calendar Start Date	Aug 28		Aug 28		Aug 28		Aug 28	
Start time	0600-0940		1000-1340		1400-1735		1800-0540	
Volume (m3)	6.75		6.75		6.60		21.5	
Stage 1 (ug/stage)	0.00	0.00	0.00	0.00	0.00	0.00	2.40	0.00
2	0.00	0.00	0.45	0.00	0.00	0.00	0.00	0.00
3	2.61	1.46	3.35	0.00	8.17	5.60	31.06	8.48
4	4.23	1.68	6.84	8.45	7.76	1.93	4.63	2.20
5	6.57	8.41	10.80	11.86	24.19	12.67	43.74	30.33
6	9.16	8.20	11.88	9.34	10.83	5.94	17.41	12.56
7	3.91	0.00	2.68	1.96	3.80	2.16	11.09	10.84
8	0.00	0.00	0.00	0.00	0.00	0.00	0.45	0.00
AF	23.60	0.70	32.50	1.40	43.85	2.00	33.50	1.90

Sample ID	CL-ER-MD-241-0558-0956		CL-ER-MD-241-1004-1340		CL-ER-MD-241-1350-1750		CL-ER-MD-241-1756-0053	
Julian Start Date	241		241		241		241	
Calendar Start Date	Aug 29		Aug 29		Aug 29		Aug 29	
Start time	0558-0956		1004-1340		1350-1750		1756-0053	
Volume (m3)	6.30		6.75		7.22		12.6	
Stage 1 (ug/stage)	0.00	0.00	0.00	0.00	0.00	0.00	0.00	0.00
2	0.00	0.00	0.00	0.00	0.00	0.00	0.00	0.25
3	5.92	3.91	17.87	3.88	0.86	2.10	2.45	3.62
4	2.87	0.53	10.69	3.89	11.40	8.36	9.41	6.77
5	11.13	8.80	15.24	4.97	17.92	6.88	18.12	12.68
6	8.94	6.42	6.55	6.40	8.83	2.88	11.43	6.13
7	2.29	2.17	5.37	1.60	2.06	2.50	11.34	6.05
8	0.00	0.00	0.00	0.00	0.00	0.00	0.00	0.00
AF	20.50	0.80	26.50	1.00	52.40	2.40	32.80	1.40

Sample ID	RB-ER-MD-241-0600-0935		RB-ER-MD-241-1000-1330		RB-ER-MD-241-1400-1740		RB-ER-MD-241-1800-0100	
Julian Start Date	241		241		241		241	
Calendar Start Date	Aug 29		Aug 29		Aug 29		Aug 29	
Start time	0600-0935		1000-1330		1400-1740		1800-0100	
Volume (m3)	6.60		6.30		6.84		12.9	
Stage 1 (ug/stage)	1.28	0.00	0.00	0.00	0.00	0.00	3.31	0.00
2	0.00	0.00	0.00	0.00	0.00	0.00	0.00	0.00
3	3.14	1.21	0.72	0.00	4.40	0.00	12.92	0.00
4	6.18	3.09	5.00	3.42	9.57	3.48	10.51	9.27
5	9.05	0.00	2.85	1.65	4.59	1.64	16.17	12.01
6	0.00	0.00	3.21	1.60	0.00	1.10	7.79	6.56
7	0.00	2.26	3.65	1.24	0.00	0.00	3.11	0.00
8	0.00	0.00	0.00	0.00	0.00	0.00	0.00	0.00
AF	22.30	0.70	22.80	0.70	25.60	2.30	27.10	1.00

Sample ID	CL-ER-MD-245-0600-0950		CL-ER-MD-245-0956-1348		CL-ER-MD-245-1353-1759		CL-ER-MD-245-1809-0554	
Julian Start Date	245		245		245		245	
Calendar Start Date	Sep 2		Sep 2		Sep 2		Sep 2	
Start time	0600-0950		0956-1348		1353-1759		1809-0554	
Volume (m3)	6.92		6.98		7.38		21.2	
Stage 1 (ug/stage)	0.00	0.00	0.00	0.00	0.00	0.00	2.05	0.00
2	0.00	0.00	0.00	0.00	0.02	0.00	0.00	0.00
3	0.00	0.00	0.00	1.75	0.00	0.00	3.08	0.00
4	0.12	1.11	10.82	1.82	1.50	1.15	2.31	4.11
5	2.95	5.01	3.57	5.53	5.56	7.03	14.20	14.70
6	0.00	1.24	1.40	3.52	13.98	8.51	21.35	18.09
7	0.00	2.80	0.00	1.33	1.20	0.00	8.19	6.83
8	0.00	0.00	2.56	0.00	0.00	0.00	1.97	2.74
AF	22.20	1.00	26.70	0.60	36.70	2.20	34.80	2.20

Sample ID	RB-ER-MD-245-0600-0935		RB-ER-MD-245-1000-1340		RB-ER-MD-245-1400-1740		RB-ER-MD-245-1800-0540	
Julian Start Date	245		245		245		245	
Calendar Start Date	Sep 2		Sep 2		Sep 2		Sep 2	
Start time	0600-0935		1000-1340		1400-1740		1800-0540	
Volume (m3)	6.69		6.75		6.75		21.8	
Stage 1 (ug/stage)	3.25	0.00	0.00	0.00	2.11	0.00	0.46	0.00
2	0.00	0.00	0.00	0.00	0.00	0.00	0.01	0.00
3	0.00	0.00	3.30	1.65	0.00	0.00	12.65	3.10
4	3.69	0.00	0.00	0.00	0.00	0.00	4.80	0.00
5	10.13	11.91	1.76	2.05	3.66	0.00	38.81	24.87
6	12.36	2.21	1.14	1.54	13.45	3.26	23.83	12.83
7	13.71	3.52	0.00	0.00	0.00	0.00	11.88	10.94
8	0.14	0.00	1.03	0.00	0.00	0.00	0.00	0.00
AF	25.00	1.20	23.90	0.40	24.50	0.80	50.75	5.15

Sample ID	CL-ER-MD-246-0601-0954		CL-ER-MD-246-1000-1349		CL-ER-MD-246-1357-1746		CL-ER-MD-246-1754-0030	
Julian Start Date	246		246		246		246	
Calendar Start Date	Sep 3		Sep 3		Sep 3		Sep 3	
Start time	0601-0954		1000-1349		1357-1746		1754-0030	
Volume (m3)	7.01		6.89		6.89		11.9	
Stage 1 (ug/stage)	0.00	0.00	0.00	0.00	0.00	0.00	0.00	0.00
2	0.00	0.00	0.00	0.00	0.00	0.00	0.00	0.00
3	2.74	2.03	2.92	0.00	0.78	0.55	0.05	0.00
4	2.56	4.99	0.00	1.99	0.00	1.08	0.35	2.05
5	17.55	9.93	22.35	16.83	5.98	3.76	2.86	2.33
6	11.16	11.68	14.41	9.46	1.09	3.56	4.20	1.96
7	4.18	6.23	4.59	1.10	1.95	2.22	0.00	0.00
8	0.00	0.00	0.00	0.00	0.00	0.00	0.00	0.00
AF	21.75	0.60	37.90	1.00	33.40	0.90	26.10	2.40

Sample ID	RB-ER-MD-246-0600-0940		RB-ER-MD-246-1000-1340		RB-ER-MD-246-1400-1740		RB-ER-MD-246-1800-0105	
Julian Start Date	246		246		246		246	
Calendar Start Date	Sep 3		Sep 3		Sep 3		Sep 3	
Start time	0600-0940		1000-1340		1400-1740		1800-0105	
Volume (m3)	6.84		6.84		6.60		13.0	
Stage 1 (ug/stage)	0.00	0.00	0.00	0.00	0.00	0.00	0.00	0.00
2	0.00	0.00	0.00	0.00	1.22	0.00	0.03	0.00
3	3.56	0.00	2.68	2.78	0.31	0.00	1.07	0.00
4	6.87	0.00	0.20	0.00	4.35	2.18	6.32	1.61
5	17.69	9.13	1.12	1.58	3.42	2.60	4.77	3.77
6	22.34	16.84	5.28	0.00	0.00	0.00	1.22	1.94
7	7.96	0.00	6.05	0.00	0.56	0.00	0.40	1.56
8	0.00	0.00	0.00	0.00	0.00	0.00	0.00	0.00
AF	26.10	1.70	37.40	1.50	37.00	1.10	28.40	0.50

Sample ID	LB-ER-MD-315-0600-0930		LB-ER-MD-315-1000-1330		LB-ER-MD-315-1400-1730		LB-ER-MD-315-1800-0530	
Julian Start Date	315		315		315		315	
Calendar Start Date	Nov 11		Nov 11		Nov 11		Nov 11	
Start time	0600-0930		1000-1330		1400-1730		1800-0530	
Volume (m3)	6.30		6.30		6.30		20.7	
Stage 1 (ug/stage)	0.00	0.00	0.56	0.00	0.30	0.00	1.09	0.00
2	0.30	0.00	0.00	0.00	0.39	0.00	2.23	0.00
3	2.87	1.32	0.18	0.00	1.01	0.00	16.04	4.36
4	3.29	2.39	3.26	1.03	3.74	1.55	19.84	5.33
5	8.55	7.84	5.32	5.30	8.33	4.63	55.42	17.55
6	9.91	9.53	5.36	2.94	7.30	4.78	66.84	19.00
7	12.39	7.97	7.09	4.06	6.00	5.03	43.32	28.68
8	4.74	0.00	0.00	0.00	1.22	0.00	9.35	1.83
AF	0.00	0.00	0.00	0.00	0.00	0.00	0.00	0.00

Sample ID	LA-ER-MD-315-0600-0930		LA-ER-MD-315-1000-1330		LA-ER-MD-315-1400-1730		LA-ER-MD-315-1800-0530	
Julian Start Date	315		315		315		315	
Calendar Start Date	Nov 11		Nov 11		Nov 11		Nov 11	
Start time	0600-0930		1000-1330		1400-1730		1800-0600	
Volume (m3)	6.30		6.30		6.30		20.7	
Stage 1 (ug/stage)	0.00	0.00	0.20	0.00	0.00	0.00	0.06	0.00
2	1.74	0.00	0.00	0.00	0.26	0.00	2.58	1.32
3	0.13	1.31	0.00	0.00	0.43	0.00	16.49	6.55
4	1.18	2.52	0.00	1.08	1.50	1.31	21.97	16.40
5	5.48	6.95	2.00	4.27	7.03	6.28	41.40	34.39
6	6.82	8.72	5.84	6.56	6.95	7.70	47.06	46.42
7	11.53	12.61	3.03	3.26	4.92	5.33	35.65	27.38
8	5.49	3.25	0.11	0.00	1.59	1.01	11.06	4.64
AF	0.00	0.00	0.00	0.00	0.00	0.00	0.00	0.00

Sample ID	LB-ER-MD-316-0600-0930		LB-ER-MD-316-1000-1330		LB-ER-MD-316-1400-1730		LB-ER-MD-316-1800-0530	
Julian Start Date	316		316		316		316	
Calendar Start Date	Nov 12		Nov 12		Nov 12		Nov 12	
Start time	0600-0930		1000-1330		1400-1730		1800-0530	
Volume (m3)	6.30		6.30		6.30		20.7	
Stage 1 (ug/stage)	0.41	0.00	0.22	0.00	0.10	0.00	8.18	3.13
2	0.16	0.00	0.00	0.00	0.00	0.00	0.29	0.00
3	4.37	2.32	2.36	0.00	2.98	0.00	3.08	1.19
4	9.04	3.32	14.66	2.09	10.46	1.66	21.46	11.85
5	27.25	19.69	28.37	9.62	13.75	10.92	53.17	19.38
6	28.86	17.28	12.64	9.57	12.93	7.29	29.83	16.62
7	20.49	7.01	3.21	3.55	4.52	4.47	32.07	8.34
8	3.41	2.25	0.00	0.00	0.00	0.00	36.13	7.47
AF	0.00	0.00	0.00	0.00	0.00	0.00	0.00	0.00

Sample ID	LA-ER-MD-316-0600-0930		LA-ER-MD-316-1000-1330		LA-ER-MD-316-1400-1730		LA-ER-MD-316-1800-0530	
Julian Start Date	316		316		316		316	
Calendar Start Date	Nov 12		Nov 12		Nov 12		Nov 12	
Start time	0600-0930		1000-1330		1400-1730		1800-0530	
Volume (m3)	6.30		6.30		6.30		20.7	
Stage 1 (ug/stage)	0.12	0.00	0.00	0.00	0.00	0.00	0.00	0.00
2	0.00	0.00	0.68	0.00	0.57	0.00	2.80	1.48
3	2.72	2.32	2.23	1.28	2.13	0.00	29.05	10.61
4	2.78	3.92	10.35	3.36	15.13	2.38	32.40	11.18
5	14.65	14.98	18.08	9.21	27.38	13.37	62.76	32.69
6	13.80	16.83	10.76	7.19	18.59	8.93	59.61	51.71
7	19.47	16.04	8.07	5.36	4.93	2.77	39.29	27.41
8	6.03	3.08	0.48	0.00	0.00	0.00	4.05	1.71
AF	0.00	0.00	0.00	0.00	0.00	0.00	0.00	0.00

Sample ID	LB-ER-MD-317-0600-0930		LB-ER-MD-317-1000-1330		LB-ER-MD-317-1400-1730		LB-ER-MD-317-1800-0000	
Julian Start Date	317		317		317		317	
Calendar Start Date	Nov 13		Nov 13		Nov 13		Nov 13	
Start time	0600-0930		1000-1330		1400-1730		1800-0000	
Volume (m3)	6.30		6.30		6.30		10.8	
Stage 1 (ug/stage)	0.00	0.00	0.35	0.00	0.84	0.00	0.00	0.00
2	0.00	0.00	0.01	0.00	0.00	0.00	0.00	0.00
3	7.17	2.47	0.00	0.00	0.12	0.73	1.30	0.00
4	9.77	5.08	6.91	2.74	2.79	1.93	4.70	1.29
5	11.44	6.10	11.91	4.65	3.27	3.69	6.37	6.33
6	3.77	4.02	1.88	1.86	0.57	1.90	1.66	1.85
7	2.86	4.73	1.42	2.52	2.03	2.75	1.66	2.07
8	0.15	0.00	0.00	0.00	0.00	0.00	0.00	0.00
AF	0.00	0.00	0.00	0.00	0.00	0.00	0.00	0.00

Sample ID	LA-ER-MD-317-0600-0930		LA-ER-MD-317-1000-1330		LA-ER-MD-317-1400-1730		LA-ER-MD-317-1800-0000	
Julian Start Date	317		317		317		317	
Calendar Start Date	Nov 13		Nov 13		Nov 13		Nov 13	
Start time	0600-0930		1000-1330		1400-1730		1800-0000	
Volume (m3)	6.30		6.30		6.30		10.8	
Stage 1 (ug/stage)	0.00	0.00	0.00	0.00	0.00	0.00	0.00	0.00
2	0.37	0.00	0.40	0.00	0.00	0.00	0.00	0.00
3	10.68	6.21	17.33	4.04	6.68	2.26	5.92	3.16
4	20.15	7.66	26.31	11.72	13.15	6.93	7.06	5.47
5	16.95	11.19	26.73	15.81	10.37	6.67	11.74	7.53
6	14.03	12.86	18.58	15.41	5.63	6.23	10.58	7.67
7	6.68	5.30	6.33	5.05	3.36	4.01	7.80	4.68
8	1.92	0.00	0.45	0.00	0.00	0.00	2.24	0.00
AF	0.00	0.00	0.00	0.00	0.00	0.00	0.00	0.00

Sample ID	LB-ER-MD-337-0600-0930		LB-ER-MD-337-1000-1330		LB-ER-MD-337-1400-1730		LB-ER-MD-337-1800-0000	
Julian Start Date	337		337		337		337	
Calendar Start Date	Dec 3		Dec 3		Dec 3		Dec 3	
Start time	0600-0930		1000-1330		1400-1730		1800-0000	
Volume (m3)	6.30		6.30		6.30		10.8	
Stage 1 (ug/stage)	0.00	0.00	0.09	0.00	0.00	0.00	0.00	0.00
2	1.77	1.36	0.58	0.00	0.70	0.00	2.62	0.00
3	72.50	31.74	23.36	5.27	12.64	0.00	38.14	16.31
4	44.35	27.49	59.57	26.50	37.09	20.27	19.57	11.21
5	56.69	32.22	37.78	27.50	30.49	22.91	48.29	22.98
6	41.32	32.15	17.06	14.87	19.10	12.68	41.24	18.05
7	19.90	12.38	5.20	6.47	4.36	5.35	31.89	12.03
8	3.50	4.23	0.00	1.06	0.00	0.00	7.43	2.29
AF	0.00	0.00	0.00	0.00	0.00	0.00	0.00	0.00

Sample ID	LA-ER-MD-337-0600-0930		LA-ER-MD-337-1000-1330		LA-ER-MD-337-1400-1730		LA-ER-MD-337-1800-0000	
Julian Start Date	337		337		337		337	
Calendar Start Date	Dec 3		Dec 3		Dec 3		Dec 3	
Start time	0600-0930		1000-1330		1400-1730		1800-0000	
Volume (m3)	6.30		6.30		6.30		10.8	
Stage 1 (ug/stage)	0.00	0.00	0.36	0.00	1.16	0.00	0.00	0.00
2	0.00	0.00	0.00	0.00	0.00	0.00	1.40	0.00
3	8.18	3.72	3.56	1.88	9.11	2.32	29.69	12.81
4	28.59	15.93	11.29	7.61	30.79	16.02	47.50	22.51
5	31.61	24.27	14.65	11.97	28.17	17.82	55.42	34.24
6	25.43	27.74	9.22	8.68	15.88	13.39	35.70	33.23
7	13.56	10.07	6.66	4.69	5.37	5.00	36.53	27.22
8	5.93	2.07	1.06	0.00	0.72	0.00	4.79	1.34
AF	0.00	0.00	0.00	0.00	0.00	0.00	0.00	0.00

Sample ID	LB-ER-MD-344-0600-0930		LB-ER-MD-344-1000-1330		LB-ER-MD-344-1400-1730		LB-ER-MD-344-1800-0530	
Julian Start Date	344		344		344		344	
Calendar Start Date	Dec 10		Dec 10		Dec 10		Dec 10	
Start time	0600-0930		1000-1330		1400-1730		1800-0530	
Volume (m3)	6.30		6.30		6.30		20.7	
Stage 1 (ug/stage)	0.00	0.00	0.00	0.00	0.00	0.00	0.00	0.00
2	1.03	0.00	0.00	0.00	0.00	0.00	2.72	0.00
3	11.43	3.94	4.71	2.38	2.60	0.00	29.39	7.34
4	25.67	10.14	11.98	7.51	4.88	1.02	37.97	9.33
5	56.52	29.19	28.58	22.63	13.04	6.49	76.71	50.15
6	29.33	19.06	17.15	13.29	11.49	7.13	95.49	22.46
7	16.83	13.01	11.64	4.08	11.68	4.76	62.04	13.91
8	3.55	1.86	0.00	0.00	0.12	0.00	18.07	4.43
AF	0.00	0.00	0.00	0.00	0.00	0.00	0.00	0.00

Sample ID	LA-ER-MD-344-0600-0930		LA-ER-MD-344-1000-1330		LA-ER-MD-344-1400-1730		LA-ER-MD-344-1800-0530	
Julian Start Date	344		344		344		344	
Calendar Start Date	Dec 10		Dec 10		Dec 10		Dec 10	
Start time	0600-0930		1000-1330		1400-1730		1800-0530	
Volume (m3)	6.30		6.30		6.30		20.7	
Stage 1 (ug/stage)	0.00	0.00	0.00	0.00	0.00	0.00	0.00	0.00
2	0.00	0.00	0.00	0.00	0.00	0.00	4.18	0.00
3	6.17	1.61	2.03	0.77	2.09	0.62	36.88	11.50
4	6.25	4.70	3.88	1.87	5.77	1.32	49.85	18.13
5	17.83	15.36	13.82	7.05	12.06	4.35	83.81	72.29
6	20.62	22.83	12.77	8.74	12.67	7.94	120.32	90.17
7	22.21	17.05	8.79	4.56	6.22	5.81	52.34	32.07
8	10.04	3.89	0.99	0.00	1.66	0.64	14.07	3.59
AF	0.00	0.00	0.00	0.00	0.00	0.00	0.00	0.00

Sample ID	LB-ER-MD-345-0600-0930		LB-ER-MD-345-1000-1330		LB-ER-MD-345-1400-1730		LB-ER-MD-345-1800-0000	
Julian Start Date	345		345		345		345	
Calendar Start Date	Dec 11		Dec 11		Dec 11		Dec 11	
Start time	0600-0930		1000-1330		1400-1730		1800-0000	
Volume (m3)	6.30		6.30		6.30		10.8	
Stage 1 (ug/stage)	0.00	0.00	0.00	0.00	0.00	0.00	1.87	1.44
2	0.04	0.00	0.00	0.00	0.00	0.00	4.73	2.27
3	11.35	5.06	1.96	2.38	6.63	4.01	28.27	18.26
4	13.96	7.62	9.29	11.27	8.99	9.67	26.33	15.37
5	22.54	17.57	12.60	15.84	14.83	13.54	13.50	30.68
6	22.84	16.52	7.74	11.18	15.53	14.94	49.20	33.91
7	13.44	13.79	4.89	7.34	10.88	11.46	47.07	31.65
8	1.16	2.10	1.44	1.40	3.27	2.48	15.96	2.19
AF	0.00	0.00	0.00	0.00	0.00	0.00	0.00	0.00

Sample ID	LA-ER-MD-345-0600-0930		LA-ER-MD-345-1000-1330		LA-ER-MD-345-1400-1730		LA-ER-MD-345-1800-0000	
Julian Start Date	345		345		345		345	
Calendar Start Date	Dec 11		Dec 11		Dec 11		Dec 11	
Start time	0600-0930		1000-1330		1400-1730		1800-0000	
Volume (m3)	6.30		6.30		6.30		10.8	
Stage 1 (ug/stage)	0.00	0.00	3.52	0.00	0.49	0.00	0.61	0.00
2	1.25	0.00	0.47	0.00	0.25	0.00	4.19	3.41
3	9.68	6.82	5.50	3.83	5.89	4.40	32.84	21.30
4	15.34	14.46	20.42	21.12	19.60	15.05	46.27	40.40
5	42.77	42.16	24.91	31.86	29.38	23.88	84.56	77.36
6	43.27	46.83	19.21	17.64	17.19	18.20	64.98	66.14
7	37.03	28.65	7.35	5.52	12.90	8.65	31.10	23.71
8	12.60	5.76	0.48	0.00	2.87	1.78	8.02	3.87
AF	0.00	0.00	0.00	0.00	0.00	0.00	0.00	0.00

APPENDIX IV

LOGNORMAL FITS TO SCAQS MOUDI DATA

All MOUDI data acquired during SCAQS were fitted with bimodal lognormal distributions. Results of the lognormal fits are provided in the following tables. Two tables (EC and ROC) are given for each of the four sites. A mass of zero in mode two indicates that data could be adequately fit with one lognormal mode.

CLAREMONT ORGANIC CARBON DATA

Julian Date	Nominal Start Time	Total Mass ($\mu g/m^3$)	Fitted Lognormal Parameters M_1	D_1	σ_1	M_2	D_2	σ_2
170	0600	12.135	10.74	0.275	1.757	1.014	1.128	1.355
170	1000	7.570	6.05	0.278	1.652	1.045	1.205	1.285
170	1400	8.123	5.083	0.244	1.603	1.46	0.713	1.506
170	1800	5.240	2.019	0.233	1.317	3.571	0.251	3.779
175	0600	8.419	3.867	0.238	1.286	3.105	0.714	1.609
175	1000	12.115	6.542	0.252	1.487	3.651	0.671	1.544
175	1400	16.190	8.807	0.238	1.391	6.564	0.669	1.384
175	1800	4.494	1.859	0.249	1.415	1.719	0.649	1.554
176	0600	14.029	8.951	0.276	1.577	3.074	0.769	1.593
176	1000	17.018	13.34	0.441	1.736	2.647	0.161	1.236
176	1400	9.526	3.2	0.241	1.27	6.061	0.378	2.554
176	1800	6.725	5.236	0.272	1.913	0.77	0.689	1.275
194	0600	12.355	7.763	0.234	1.397	3.539	0.655	1.326
194	1000	11.221	7.273	0.243	1.367	3.481	0.582	1.408
194	1400	10.239	7.853	0.231	1.445	1.854	0.559	1.394
194	1800	4.725	3.132	0.229	1.558	0.962	0.674	1.298
195	0600	6.684	4.788	0.211	1.554	1.791	0.566	1.441
195	1000	7.763	5.452	0.262	1.528	2.175	0.647	1.34
195	1400	9.324	2.893	0.234	1.264	6.354	0.416	2.064
195	1800	3.929	1.367	0.625	1.548	2.621	0.283	2.307
196	0600	6.385	3.117	0.219	1.334	3.394	0.564	1.713
196	1000	10.525	5.352	0.67	1.311	4.459	0.3	1.405
196	1400	7.508	7.708	0.383	1.938	0	0	0
196	1800	6.141	3.177	0.258	1.329	2.275	0.618	1.395
239	0600	4.468	0.764	0.19	1.244	3.411	0.313	1.634
239	1000	4.091	2.779	0.18	1.243	1.276	0.238	1.361
239	1400	9.542	2.06	0.192	1.264	7.807	0.341	1.626
239	1800	3.989	2.452	0.393	1.442	1.109	0.146	1.406
240	0600	3.706	3.233	0.248	1.598	0.679	1.245	1.249
240	1000	5.857	3.214	0.577	1.415	2.758	0.233	1.426
240	1400	9.607	9.329	0.28	1.435	0.802	1.244	1.25
240	1800	4.886	1.675	0.279	1.379	2.962	0.388	1.833
241	0600	4.945	3.603	0.274	1.342	1.416	1.188	1.333
241	1000	8.845	3.123	1.225	1.249	6.218	0.369	2.006
241	1400	6.520	3.291	0.274	1.293	3.319	0.599	1.395
241	1800	4.187	1.53	0.26	1.239	2.004	0.535	1.656
245	0600	0.486	0.554	0.395	1.246	0	0	0
245	1000	2.912	2.183	0.714	1.261	1.244	0.029	1.319
245	1400	3.532	0.989	0.276	1.178	2.242	0.24	1.133
245	1800	2.568	1.671	0.238	1.236	0.822	0.411	2.766
246	0600	6.061	5.595	0.29	1.457	0.607	1.208	1.292
246	1000	7.026	6.915	0.29	1.414	0.601	1.242	1.261
246	1400	1.555	1.085	0.402	1.227	0.433	0.155	1.202
246	1800	0.629	0.450	0.249	1.161	0.170	0.301	1.237

CLAREMONT ELEMENTAL CARBON DATA

Julian Date	Nominal Start Time	Total Mass ($\mu g/m^3$)	Fitted Lognormal Parameters M_1	D_1	σ_1	M_2	D_2	σ_2
170	0600	3.349	2.789	0.219	1.455	0.439	0.591	1.347
170	1000	2.117	1.05	0.216	1.316	1.137	0.378	1.644
170	1400	1.688	1.72	0.298	1.495	0	0	0
170	1800	1.721	1.372	0.22	1.583	0.116	0.565	1.327
175	0600	3.475	1.773	0.233	1.363	1.585	0.786	1.768
175	1000	4.249	0.819	0.247	1.263	3.369	0.38	2
175	1400	3.740	1.676	0.257	1.368	1.847	0.592	1.574
175	1800	1.706	1.107	0.215	1.362	0.411	0.688	1.288
176	0600	6.281	2.172	0.239	1.253	3.959	0.31	1.978
176	1000	4.500	1.998	0.254	1.273	2.526	0.433	1.752
176	1400	3.256	1.537	0.239	1.247	1.817	0.375	1.688
176	1800	1.575	1.209	0.234	1.457	0.303	0.607	1.359
194	0600	3.916	3.154	0.226	1.539	0.487	0.635	1.345
194	1000	2.834	1.482	0.202	1.305	1.441	0.332	1.581
194	1400	2.198	2.357	0.267	1.638	0	0	0
194	1800	0.818	0.682	0.179	1.572	0.125	0.663	1.311
195	0600	2.125	1.107	0.195	1.293	1.102	0.35	1.642
195	1000	2.589	1.259	0.198	1.323	1.471	0.494	1.559
195	1400	2.940	1.532	0.241	1.234	1.486	0.372	1.673
195	1800	0.956	0.326	.0211	1.355	0.653	0.528	1.65
196	0600	1.691	1.03	0.245	1.301	0.661	0.387	1.352
196	1000	2.414	1.418	0.256	1.293	1.074	0.596	1.406
196	1400	1.664	1.712	0.309	1.664	0	0	0
196	1800	1.445	0.937	0.24	1.315	0.553	0.585	1.423
239	0600	3.436	1.926	0.172	1.236	1.494	0.333	1.368
239	1000	2.335	2.308	0.225	1.181	0	0	0
239	1400	2.883	2.016	0.281	1.205	0.984	0.419	1.422
239	1800	1.132	0.827	0.256	1.162	0.525	0.027	1.328
240	0600	2.991	2.444	0.255	1.233	0.64	1.258	1.243
240	1000	3.557	2.685	0.442	1.236	0.858	0.147	1.18
240	1400	2.253	1.674	0.258	1.185	0.614	.338	1.307
240	1800	2.938	3.012	0.26	1.548	0	0	0
241	0600	3.465	2.871	0.279	1.399	0.736	1.287	1.222
241	1000	3.292	1.901	0.248	1.234	1.484	0.958	1.514
241	1400	3.606	2.795	0.614	1.537	0.888	0.187	1.308
241	1800	2.817	2.542	0.347	1.908	0.250	1.169	1.293
245	0600	1.613	0.996	0.428	1.264	0.616	0.155	1.198
245	1000	2.215	1.716	0.286	1.459	0.587	1.017	1.523
245	1400	2.650	0.666	0.319	1.254	1.933	0.258	0.862
245	1800	2.245	1.217	0.241	1.215	0.935	0.359	1.844
246	0600	5.532	2.989	0.223	1.272	2.79	0.496	2.067
246	1000	4.664	2.93	0.28	1.211	1.74	0.395	1.383
246	1400	1.773	0.896	0.213	1.331	0.872	0.373	1.711
246	1800	0.534	0.332	0.268	1.210	0.235	0.700	1.283

RUBIDOUX ORGANIC CARBON DATA

Julian Date	Nominal Start Time	Total Mass ($\mu g/m^3$)	Fitted Lognormal Parameters M_1	D_1	σ_1	M_2	D_2	σ_2
170	0600	7.543	4.372	0.182	1.576	3.239	0.645	1.854
170	1000	4.720	2.295	0.277	1.369	2.579	1.565	1.655
170	1400	2.726	2	0.273	1.229	0.716	1.225	1.274
170	1800	2.002	1.56	0.281	1.262	0.471	1.343	1.39
175	0600	6.373	3.925	1.077	1.509	2.384	0.226	1.29
175	1000	12.007	4.841	1.246	1.269	7.028	0.336	1.687
175	1400	5.327	2.416	1.307	1.206	2.712	0.363	1.316
175	1800	2.871	1.309	0.197	1.535	1.448	0.676	1.838
176	0600	2.993	1.508	0.225	1.145	1.362	1.023	1.381
176	1000	5.665	3.853	0.859	1.395	1.668	0.265	1.204
176	1400	5.143	3.021	0.281	1.233	1.858	0.026	1.334
176	1800	4.544	2.833	0.263	1.393	1.604	1.177	1.343
194	0600	8.067	4.047	0.235	1.289	3.501	0.887	1.609
194	1000	3.508	2.508	0.324	1.351	1.113	0.847	1.656
194	1400	4.735	3.216	0.319	1.3	1.113	0.935	1.609
194	1800	2.930	2.493	0.241	1.473	0.412	0.53	1.381
195	0600	4.501	3.684	0.361	1.98	0.657	4.447	1.309
195	1000	4.182	1.883	0.245	1.317	2.299	0.63	1.643
195	1400	3.198	1.241	0.300	1.251	2.128	0.575	1.657
195	1800	2.583	1.415	0.717	1.527	0.941	0.248	1.46
196	0600	2.928	2.198	0.716	1.662	0.621	0.206	1.613
196	1000	8.047	6.058	0.783	1.46	1.411	0.238	1.389
196	1400	4.095	2.961	0.387	1.293	1.43	0.13	1.374
196	1800	2.927	1.544	0.264	1.206	1.409	0.728	1.282
239	0600	6.880	3.11	0.648	0.648	1.356	4.198	1.741
239	1000	5.414	3.695	0.65	1.529	1.79	0.233	2.169
239	1400	6.836	4.516	0.25	1.242	1.886	0.664	1.343
239	1800	4.430	3.02	0.27	1.503	1.433	0.828	1.651
240	0600	4.203	2.551	0.226	1.3	1.668	0.756	1.711
240	1000	5.714	3.292	0.245	1.242	2.432	0.723	1.628
240	1400	8.691	6.94	0.336	1.534	1.846	1.181	1.304
240	1800	5.128	3.12	0.336	1.412	1.647	1.297	1.21
241	0600	3.119	1.817	0.427	1.356	1.322	0.907	1.465
241	1000	2.449	1.094	0.705	1.299	1.404	0.179	1.574
241	1400	2.945	2.935	0.758	1.508	.145	0.307	1.202
241	1800	4.270	1.404	1.176	1.304	2.727	0.354	1.707
245	0600	6.870	4.422	0.163	1.484	2.314	0.418	1.669
245	1000	1.147	0.587	0.033	1.262	0.62	1.288	1.221
245	1400	2.913	0.699	0.265	1.18	1.986	0.231	0.879
245	1800	4.279	3.567	0.294	1.528	0.686	1.276	1.223
246	0600	9.272	4.868	0.235	1.245	4.815	0.457	2.342
246	1000	2.433	2.027	0.167	1.392	0.498	1.294	1.217
246	1400	1.565	1.0	1.113	1.179	1.296	0.589	1.334
246	1800	1.095	1.36	0.243	1.164	0.601	0.776	1.223

RUBIDOUX ELEMENTAL CARBON DATA

Julian Date	Nominal Start Time	Total Mass ($\mu g/m^3$)	Fitted Lognormal Parameters M_1	D_1	σ_1	M_2	D_2	σ_2
170	0600	2.382	2.069	0.204	1.663	0.416	0.573	1.429
170	1000	1.242	0.939	0.269	1.21	0.382	0.613	1.426
170	1400	0.595	0.278	0.381	1.351	0.37	0.276	1.208
170	1800	0.394	0.243	0.138	1.417	0.18	0.353	1.376
175	0600	2.207	01.506	0.179	1.653	0.843	0.828	1.71
175	1000	5.971	02.743	0.27	1.281	3.448	0.753	1.761
175	1400	1.700	01.379	0.323	1.536	0.292	1.243	1.247
175	1800	1.614	0.803	0.243	1.278	0.867	0.496	2.204
176	0600	2.538	01.851	0.222	1.362	0.685	1.046	1.539
176	1000	2.516	01.252	0.264	1.207	1.307	0.739	1.292
176	1400	1.570	0.927	0.277	1.23	0.735	0.849	1.612
176	1800	1.605	0.916	0.236	1.316	0.666	0.665	1.467
194	0600	4.441	02.426	0.232	1.364	2.094	0.896	1.616
194	1000	0.683	0.477	0.274	1.207	0.272	0.385	1.381
194	1400	0.332	0.383	0.395	1.266	0	0	0
194	1800	1.292	01.182	0.199	1.628	0.158	0.541	1.428
195	0600	3.461	03.631	0.207	1.634	0	0	0
195	1000	2.818	02.204	0.386	1.422	0.631	0.145	1.424
195	1400	3.199	1.195	0.297	1.244	2.096	0.556	1.608
195	1800	1.407	0.576	0.686	1.32	0.843	0.224	1.646
196	0600	1.799	0.906	0.283	1.247	0.999	0.932	1.532
196	1000	3.189	2.014	0.702	1.303	01.228	0.278	1.235
196	1400	1.742	1.496	0.393	1.276	0.282	0.142	1.455
196	1800	1.878	1.129	0.277	1.228	0.871	0.661	1.332
239	0600	4.313	4.783	0.196	1.822	0	0	0
239	1000	1.366	1.202	0.439	1.304	0.255	0.116	1.257
239	1400	3.044	2.393	0.255	1.189	0.808	0.722	1.258
239	1800	2.345	1.757	0.21	1.374	0.536	0.685	1.417
240	0600	3.136	0.659	0.374	1.374	2.192	0.262	1.19
240	1000	5.018	2.947	0.257	1.266	2.228	0.64	1.36
240	1400	4.492	3.432	0.32	1.454	1.075	1.268	1.234
240	1800	2.982	2.237	0.337	1.452	0.449	1.286	1.214
241	0600	1.041	0.731	0.814	1.326	0.414	0.108	1.207
241	1000	1.256	0.707	0.705	1.268	0.6	0.207	1.492
241	1400	0.988	0.704	0.714	1.257	0.35	0.267	1.217
241	1800	2.210	1.222	0.28	1.235	1.131	0.661	1.329
245	0600	2.800	2.23	0.4	1.261	0.798	0.13	1.275
245	1000	0.831	0.584	0.281	1.239	0.313	1.283	1.225
245	1400	0.494	0.427	0.218	1.126	0.119	0.247	1.164
245	1800	2.395	1.284	0.374	1.316	1.132	0.171	1.52
246	0600	4.122	1.266	0.287	1.21	3.025	0.243	1.152
246	1000	0.692	0.508	1.305	1.209	0.291	0.391	1.246
246	1400	0.759	0.864	0.531	1.516	0	0	0
246	1800	0.704	0.608	0.392	1.717	0.141	0.143	1.416

LONG BEACH ORGANIC CARBON DATA

Julian Date	Nominal Start Time	Total Mass ($\mu g/m^3$)	Fitted Lognormal Parameters M_1	D_1	σ_1	M_2	D_2	σ_2
315	0600	5.197	3.508	0.23	1.482	1.547	0.059	1.563
315	1000	2.385	2.096	0.199	1.676	0.356	0.647	1.334
315	1400	3.075	2.407	0.243	1.449	0.592	0.593	1.367
315	1800	9.376	4.554	0.237	1.258	5.291	0.435	3.343
316	0600	8.233	5.319	0.235	1.261	8.016	0.301	2.123
316	1000	3.941	4.146	0.285	1.249	4.52	0.556	1.44
316	1400	3.863	3.452	0.253	1.235	2.42	0.652	1.41
316	1800	3.147	4.636	0.041	1.439	4.897	0.322	1.557
317	0600	4.367	3.154	0.462	1.593	1.191	1.148	1.331
317	1000	2.572	1.398	0.391	1.278	1.379	0.596	1.396
317	1400	0.570	0.531	0.51	1.437	0.095	0.116	1.303
317	1800	1.453	1.341	0.493	1.698	0.127	0.124	1.396
337	0600	36.434	18.038	1.153	1.355	19.313	0.286	1.515
337	1000	21.503	16.35	0.739	1.463	5.236	0.268	1.256
337	1400	15.266	6.101	0.272	1.233	9.233	0.739	1.407
337	1800	17.52	11.132	0.263	1.517	5.101	1.201	1.309
344	0600	21.321	7.788	0.279	1.387	13.136	0.485	1.915
344	1000	10.565	2.542	0.263	1.33	8.017	0.376	1.909
344	1400	5.746	4.87	0.235	1.598	0.771	0.691	1.557
344	1800	14.438	8.237	0.234	1.287	4.743	0.745	1.81
345	0600	12.163	6.898	0.239	1.318	5.211	0.792	1.729
345	1000	4.600	2.67	0.269	1.408	1.892	0.639	1.345
345	1400	8.116	2.999	0.236	1.249	5.814	0.552	3.083
345	1800	17.31	8.267	0.210	1.246	5.305	0.979	1.462

LONG BEACH ELEMENTAL CARBON DATA

Julian Date	Nominal Start Time	Total Mass ($\mu g/m^3$)	Fitted Lognormal Parameters M_1	D_1	σ_1	M_2	D_2	σ_2
315	0600	4.611	2.07	0.228	1.284	2.926	0.263	2.727
315	1000	2.114	0.93	0.383	1.395	1.236	0.171	1.679
315	1400	2.538	2.156	0.222	1.53	0.34	0.627	1.332
315	1800	3.554	3.218	0.198	1.743	0.4	1.038	1.493
316	0600	8.233	3.441	0.251	1.223	3.891	0.336	1.597
316	1000	3.941	1.937	0.246	1.218	2.007	0.342	1.667
316	1400	3.863	3.316	0.272	1.455	0.439	0.501	1.401
316	1800	3.147	1.878	0.27	1.355	0.869	0.043	1.305
317	0600	3.555	2.066	0.223	1.679	1.548	0.759	1.597
317	1000	1.867	1.454	0.456	1.639	0.532	0.143	1.552
317	1400	1.747	1.41	0.381	1.893	0.353	0.127	1.487
317	1800	1.06	0.780	0.391	1.350	0.289	0.151	1.535
337	0600	22.470	10.324	0.252	1.268	11.533	0.98	1.548
337	1000	12.963	7.037	0.662	1.402	5.496	0.264	1.326
337	1400	9.716	4.996	0.268	1.348	4.921	0.649	1.338
337	1800	7.395	4.946	0.271	1.509	2.510	1.138	1.378
344	0600	12.253	3.708	0.26	1.329	8.215	0.369	2.004
344	1000	7.920	3.164	0.267	1.26	4.675	0.434	1.693
344	1400	3.080	2.576	0.238	1.364	0.367	0.516	1.314
344	1800	4.983	4.091	0.325	1.465	0.461	1.2	1.276
345	0600	9.946	3.508	0.237	1.297	7.211	0.394	3.122
345	1000	7.843	4.142	0.249	1.369	3.153	0.646	1.429
345	1400	8.905	4.948	0.23	1.332	3.082	0.709	1.55
345	1800	12.571	8.464	0.228	1.493	3.577	1.027	1.525

LOS ANGELES ORGANIC CARBON DATA

Julian Date	Nominal Start Time	Total Mass ($\mu g/m^3$)	Fitted Lognormal Parameters M_1	D_1	σ_1	M_2	D_2	σ_2
315	0600	3.739	4.007	0.131	2.15	0	0	0
315	1000	1.010	0.987	0.205	1.188	0	0	0
315	1400	2.300	2.363	0.246	1.568	0	0	0
315	1800	7.672	4.928	0.221	1.493	2.179	0.828	1.629
316	0600	8.008	6.201	0.147	1.789	1.685	0.364	1.343
316	1000	6.666	7.816	0.365	2.216	0	0	0
316	1400	9.628	5.521	0.262	1.268	4.269	0.591	1.414
316	1800	10.161	6.985	0.236	1.552	3.232	0.924	1.583
317	0600	9.747	5.951	0.762	1.537	3.775	0.235	1.328
317	1000	13.934	4.982	0.25	1.296	9.379	0.779	1.661
317	1400	5.030	3.658	0.739	1.53	1.406	0.248	1.397
317	1800	4.198	2.572	0.239	1.564	1.421	0.915	1.566
337	0600	16.553	7.994	0.241	1.372	7.397	0.68	1.416
337	1000	6.012	2.118	0.69	1.389	3.908	0.265	1.683
337	1400	12.987	8.05	0.687	1.422	4.857	0.261	1.316
337	1800	19.54	11.768	0.745	1.837	8.794	0.188	1.732
344	0600	11.765	8.392	0.223	1.656	2.779	0.058	1.585
344	1000	5.364	0.721	0.226	1.268	4.69	0.264	1.757
344	1400	4.994	3.425	0.235	1.335	1.452	0.575	1.448
344	1800	16.248	9.527	0.228	1.29	5.996	0.785	1.76
345	0600	24.078	18.114	0.228	1.626	4.322	0.866	1.719
345	1000	11.416	5.649	0.249	1.322	5.343	0.658	1.422
345	1400	12.511	14.923	0.4	2.477	0	0	0
345	1800	25.18	7.524	0.243	1.305	18.504	0.556	2.428

LOS ANGELES ELEMENTAL CARBON DATA

Julian Date	Nominal Start Time	Total Mass ($\mu g/m^3$)	Fitted Lognormal Parameters M_1	D_1	σ_1	M_2	D_2	σ_2
315	0600	5.613	5.053	0.164	1.905	.67	0.792	1.661
315	1000	2.406	1.971	0.223	1.335	.387	0.55	1.405
315	1400	3.433	2.86	0.224	1.478	.349	0.583	1.332
315	1800	6.347	4.242	0.22	1.372	1.662	0.661	1.573
316	0600	9.075	4.099	0.218	1.494	5.932	0.201	3.409
316	1000	4.190	3.034	0.232	1.653	1.24	0.584	1.798
316	1400	4.357	1.029	0.249	1.236	3.33	0.33	1.561
316	1800	6.333	4.497	0.22	1.345	1.669	0.769	1.877
317	0600	6.860	3.808	0.232	1.323	3.133	0.822	1.679
317	1000	8.259	4.398	0.239	1.289	3.804	0.673	1.536
317	1400	4.144	2.191	0.22	1.443	1.916	0.715	1.439
317	1800	2.690	1.482	0.220	1.421	1.188	0.750	1.663
337	0600	13.300	7.963	0.236	1.29	4.751	0.651	1.458
337	1000	5.529	3.244	0.243	1.458	2.227	0.65	1.459
337	1400	8.659	4.529	0.249	1.355	4.044	0.664	1.355
337	1800	12.08	7.501	0.207	1.550	4.88	0.743	1.687
344	0600	10.387	7.99	0.213	1.446	1.428	0.655	1.464
344	1000	3.648	1.671	0.226	1.286	2.074	0.303	2.127
344	1400	3.282	2.685	0.205	1.419	.446	0.686	1.54
344	1800	10.544	5.86	0.236	1.261	4.622	0.388	2.112
345	0600	22.965	8.452	0.228	1.298	14.724	0.318	2.401
345	1000	12.693	6.302	0.264	1.351	6.291	0.625	1.43
345	1400	11.421	5.991	0.242	1.379	4.938	0.638	1.519
345	1800	21.87	7.918	0.241	1.265	14.149	0.521	2.13